

The coactivator role of histone deacetylase 3 in IL-1-signaling involves deacetylation of p65 NF- κ B

Elisabeth Ziesché¹, Daniela Kettner-Buhrow¹, Axel Weber¹, Tobias Wittwer², Liane Jurida¹, Johanna Soelch¹, Helmut Müller¹, Doris Newel¹, Petra Kronich¹, Heike Schneider³, Oliver Dittrich-Breiholz³, Srividya Bhaskara⁴, Scott W. Hiebert⁴, Michael O. Hottiger⁵, Haiying Li⁶, Ezra Burstein^{6,7}, M. Lienhard Schmitz^{2,*} and Michael Kracht^{1,*}

¹Rudolf-Buchheim-Institute of Pharmacology, ²Institute of Biochemistry, Justus-Liebig-University Giessen, D-35392 Giessen, ³Institute of Biochemistry, Hannover Medical School, D-30625 Hannover, Germany, ⁴Vanderbilt-Ingram Cancer Center, Vanderbilt University School of Medicine, Nashville, TN 37232, USA, ⁵Institute of Veterinary Biochemistry and Molecular Biology, University of Zurich, 8057 Zurich, Switzerland, ⁶Departments of Internal Medicine and ⁷Molecular Biology, UT Southwestern Medical Center, Dallas, Texas 75390, USA

Received May 30, 2012; Revised September 7, 2012; Accepted September 11, 2012

ABSTRACT

Histone deacetylase (HDAC) 3, as a cofactor in co-repressor complexes containing silencing mediator for retinoid or thyroid-hormone receptors (SMRT) and nuclear receptor co-repressor (N-CoR), has been shown to repress gene transcription in a variety of contexts. Here, we reveal a novel role for HDAC3 as a positive regulator of IL-1-induced gene expression. Various experimental approaches involving RNAi-mediated knockdown, conditional gene deletion or small molecule inhibitors indicate a positive role of HDAC3 for transcription of the majority of IL-1-induced human or murine genes. This effect was independent from the gene regulatory effects mediated by the broad-spectrum HDAC inhibitor trichostatin A (TSA) and thus suggests IL-1-specific functions for HDAC3. The stimulatory function of HDAC3 for inflammatory gene expression involves a mechanism that uses binding to NF- κ B p65 and its deacetylation at various lysines. NF- κ B p65-deficient cells stably reconstituted to express acetylation mimicking forms of p65 (p65 K/Q) had largely lost their potential to stimulate IL-1-triggered gene expression, implying that the co-activating property of HDAC3 involves the

removal of inhibitory NF- κ B p65 acetylations at K122, 123, 314 and 315. These data describe a novel function for HDAC3 as a co-activator in inflammatory signaling pathways and help to explain the anti-inflammatory effects frequently observed for HDAC inhibitors in (pre)clinical use.

INTRODUCTION

Pathogen-associated molecular patterns or damage/danger-associated molecular patterns are sensed by specific receptors, which in turn activate signaling cascades to induce the synthesis of inflammatory mediators such as tumor necrosis factor (TNF) or interleukin(IL)-1 and IL-8 (1). Once released, these cytokines in turn stimulate their cognate receptors and thus mediate the rapid amplification of the inflammatory response. One central inducible transcription factor system of major importance for the pro-inflammatory gene expression program is NF- κ B (2). It consists of five different DNA-binding subunits that occur in different dimer combinations, but a heterodimer between p50 and the strongly transactivating p65 subunit is the most frequently detected form (3). The DNA-binding NF- κ B dimer is retained in the cytosol by association with an inhibitory I κ B protein, thus maintaining this transcription factor in an inactive status. A plethora of damage/danger-associated molecular pattern signals

*To whom correspondence should be addressed. Tel: +49 0641 99 47600; Fax: +49 0641 99 47619;

Email: Michael.Kracht@pharma.med.uni-giessen.de

Correspondence may also be addressed to M. Lienhard Schmitz. Tel: +49 0641 99 47570; Fax: +49 0641 99 47589;

Email: lienhard.schmitz@biochemie.med.uni-giessen.de

The authors wish to be known that, in their opinion, the first three authors should be regarded as joint First Authors.

ranging from proinflammatory signals to toxic, physical and oxidative stresses leads to the phosphorylation and degradation of I κ B and thus allow subsequent nuclear translocation of the DNA-binding subunits and inducible gene expression (2,4).

Specificity in NF- κ B-triggered gene expression is achieved by several mechanisms mainly occurring in the nucleus. These include the generation of distinct DNA-binding dimers, interplay between NF- κ B and other transcription factors, stimulus-specific modification and remodeling of chromatin and by posttranslational modifications (PTMs) of the DNA-binding subunits (4,5). Although PTMs were reported for all five members of the NF- κ B family, most information has been gathered for the p65 subunit, which is modified by phosphorylation, monomethylation, degradative and regulatory ubiquitination, as well as acetylation (6–8). Historically, most of the PTMs were considered to exert stimulatory functions, but the underlying evidence is mainly based on the use of synthetic reporter genes and overexpression systems. Reconstitution of p65-deficient cells with p65 variants mutated at individual sites of modification has recently revealed a more complex picture and showed that the outcome of a given PTM is highly target gene specific. This is exemplified by p65 acetylation, which occurs at several lysines. Although an inhibitory function has been reported for acetylation at lysines 122 and 123 (9), overexpression experiments revealed a stimulatory function for acetylation of lysine 310 (10,11). Reconstitution experiments showed that the recently discovered acetylation sites at lysines 314 and 315 serve to augment or to dampen NF- κ B-dependent transcription in a target gene-specific manner (12–14).

The regulation of p65 acetylation is achieved by several mechanisms. As acetylation and ubiquitination use an overlapping set of lysines (123, 310 and 314), both competing PTMs were found to inhibit each other (15). Acetylation of p65 occurs by the histone acetyltransferases (HATs) CREB-binding protein (CBP)/p300 but also by p300/CBP-associated factor (PCAF) (9,16–19). Deacetylation of p65 can be mediated by the histone deacetylases (HDACs) HDAC1, HDAC2 and HDAC3, which all belong to the class I family of HDACs with homology to the budding yeast counterparts Rpd3 (9,19–21). The class III HDACs, SIRT1 and SIRT2, can also deacetylate p65 (13,22). HDACs are typically found in large high molecular weight complexes that often contain other HDACs or accessory proteins important for the regulation of chromatin, gene expression, RNA splicing or further functions (21,23).

HDAC3 deacetylates histones *in vitro* (24) and has been purified as a catalytic subunit of SMRT-NCoR containing nuclear complexes, which mediate nuclear hormone receptor-dependent transcriptional repression (23,25,26). These initial observations and follow-up studies have firmly established HDAC3 as a transcriptional co-repressor (27). However, HDAC3 is also present in the cytoplasm (28) and was found to deacetylate a variety of protein substrates, suggesting that its physiological functions may reach beyond its role as a co-repressor (27).

The high number of HDAC3 target proteins also explains the importance of HDAC3 for several epigenetic and genetic fundamental processes. Targeted deletion of HDAC3 showed its contribution to the maintenance of chromatin structure, genome stability and the cell cycle (29,30). In addition, organ-specific deletion revealed its role in cardiac energy metabolism (31), metabolic transcription networks in the liver (32) and as a critical regulator of S phase progression and DNA damage control (33).

Here, we show that the reported anti-inflammatory effects of HDAC inhibitors (34) are at least, in part, owing to the stimulatory role of HDAC3 for IL-1-induced gene expression. A variety of biochemical, pharmacological and genetic approaches showed an important role of HDAC3 for efficient expression of IL-1 target genes. This effect is mainly mediated by the HDAC3-mediated deacetylation of NF- κ B p65 at lysines 122, 123, 314 and 315.

MATERIALS AND METHODS

Cells and materials

HEK293 cells stably expressing the IL-1 receptor (HEK293IL-1R) (35), human epithelial carcinoma KB cells (36), A549 lung epithelial carcinoma cells (catalogue number ACC 107, German Collection of Microorganisms and Cell Cultures), mouse embryonic fibroblasts (Mefs) with a tamoxifen-inducible deletion of HDAC3 (33), p65 NF- κ B-deficient and reconstituted Mefs (15), and all other Mefs lines were cultured in Dulbecco's modified Eagle's medium, complemented with 10% fetal calf serum, 2 mM L-glutamine, 100 U/ml penicillin and 100 μ g/ml streptomycin. For the experiments shown in Figure 2 and Supplementary Figures S3, S6, S10, S11, *Hdac3*^{fl/+} or *Hdac3*^{fl/-} Mefs were immortalized by the 3T3 protocol. For the experiments shown in Supplementary Figure S2, wild-type Mef lines obtained from Matthias Gaestel (37) and from Mitchell A. Lazar (38) were used.

Antibodies against the following proteins or peptides were used: β -actin (JLA20; EMD), p65 (C-20, sc-372), HDAC1 (C-19, sc-6298), HDAC3 (H-99, sc-11417), p300 (N15, sc-584) and mouse IgG (sc-2025) from Santa Cruz; GFP (clone 7.1 and 13.1; 11814460001) and MYC (9E10) from Roche; acetyl-NF- κ B p65 (K310) (3045) and acetylated lysine antibody (9441) from Cell Signaling; acetyl-histone H3 (K9/14) (06-599; Upstate), acetyl-NF- κ B p65 (K310) (ab52175) from Abcam; FLAG (clone M2; F1804) and β -tubulin (clone TUB2.1; T4026) from Sigma and HDAC3 (mouse monoclonal: MCA4831Z; AbD Serotec). Antibodies against acetyl-NF- κ B p65 (K314) and acetyl-NF- κ B p65 (K315) were generated by Michael O. Hottiger and have been described in (12,14).

TSA, apicidin, tamoxifen and puromycin were from Sigma. Human recombinant IL-1 α was used at 10 ng/ml in all experiments and was a kind gift from Jeremy Saklatvala, London, UK. Recombinant human TNF α was from R&D Systems or Hoelzel. Ni²⁺-NTA agarose was from Qiagen (1018244), and True Blot anti-mouse Ig IP beads were from eBioscience (00-8811-25).

Plasmids, transfections, reporter gene assays and selection of stable cell lines

For reporter gene assays the following expression vectors were used: pUHC13-3-IL-8 promoter and pSV40- β -galactosidase (SV40- β -gal) (39). His-p65, YFP (yellow fluorescent protein)-CBP, HA-p65 and its various point mutated derivatives (HA-p65 K310Q / K310R, HA-p65 K4Q / K4R, HA-p65 K5Q / K5R) were described (15). Additional K-Q mutants of p65, His-p65 E39I and His-p65 K5R were generated by site-directed mutagenesis as described (40). HDAC3-HA was a kind gift of Dr. Edward Seto, Tampa, Florida. Expression vectors for p300, HDAC1, HDAC2, HDAC5, HDAC8 have been described.

Transient transfections by the calcium phosphate method and determination of luciferase reporter gene activity were performed as described previously (40). Equal amounts of plasmid DNA within each experiment were obtained by adding empty vector.

For establishing a stable knockdown of HDAC3, HEK293IL-1R cells were transfected with Sure SilencingTM shRNA plasmids against human HDAC3 (clone ID3) (Superarray Biosciences; KH05911P) or an empty control vector (pSuper-Puro) as negative control, using the calcium phosphate method. Twenty-four hours post transfection, selection was started using 0.75 μ g/ml puromycin, and stable cell lines were isolated. KB cells were stably transfected with the same plasmids using Lipofectamine (InvitrogenTM) and also selected in 0.75 μ g/ml puromycin.

Cell lysis and coimmunoprecipitation

HEK293IL-1R cell lines with a partial shRNA-mediated knockdown of HDAC3 (Figure 1A) were harvested after washing in cold phosphate-buffered saline (PBS) and collected by centrifugation. The pellet was directly lysed in a modified lysis buffer (50 mM HEPES pH 7.4, 250 mM NaCl, 1 mM EDTA, 1% NP-40, 2 mM Na₃VO₄, 50 mM NaF, 20 mM β -glycerophosphate, 4 μ M TSA, 1 mM PMSF, 1 \times protease inhibitor cocktail from Roche (11697498001) containing TSA for inhibiting HDAC. After rotating for 30 min at 4°C, the lysates were centrifuged (15 min, 13 000 r.p.m., 4°C) and used for Western blotting or were stored frozen.

Transiently transfected HEK293IL-1R cells (Figures 1D and E, 3B, 5B and C) were harvested after washing in cold PBS and collected by centrifugation. The pellet was directly lysed in β -galactosidase lysis buffer as described (36).

Mefs with a tamoxifen-inducible deletion of HDAC3 (Figure 2A) were harvested after washing in cold PBS and collected by centrifugation. The pellet was directly lysed in cell lysis buffer (10 mM Tris pH 7.05, 30 mM Na₄O₇P₂ \times 10H₂O, 50 mM NaCl, 1% Triton X-100, 2 mM Na₃VO₄, 50 mM NaF, 20 mM β -glycerophosphate, 1 μ g/ml pepstatin, 10 μ g/ml leupeptin, 1 mM PMSF, 1 μ M microcystin), incubated for 15 min on ice, and, after centrifugation, the lysate was further used for Western blotting.

For coimmunoprecipitation experiments (Figure 4B), cells were harvested after washing in PBS and collected by centrifugation. The pellet was directly lysed in cell lysis buffer (50 mM HEPES pH 7.4, 50 mM NaCl, 1% Tween20, 2.5 mM EGTA, 1 mM EDTA, 1 mM NaF, 10 mM β -glycerophosphate, 0.1 mM Na₃VO₄, 1 mM PMSF, 1 mM DTT, 1 \times protease inhibitor cocktail from Roche) and incubated for 20 min on ice. The DNA was sheared by three sonication steps of 20 s, and lysates were cleared by ultracentrifugation for 20 min at 100.000g and 4°C. HDAC3 was immunoprecipitated from 0.5 mg precleared cell extracts using 2 μ g mouse monoclonal anti-HDAC3 antibody (AbD Serotec) or 2 μ g normal mouse IgG (Santa Cruz) coupled for 2 h to 25 μ l True Blot anti-mouse Ig IP beads (eBioscience). After rotating for 2 h at 4°C, the supernatant was discarded, and the beads were washed three times with high salt wash buffer (50 mM HEPES pH 7.4, 450 mM NaCl, 1% Tween20, 2.5 mM EGTA, 1 mM EDTA, 1 mM NaF, 10 mM β -glycerophosphate, 0.1 mM Na₃VO₄, 1 mM PMSF, 1 mM DTT, 1 \times protease inhibitor cocktail from Roche). The precipitated proteins were eluted by boiling in 2 \times Roti-Load for 10 min before analyzing by western blotting.

NF- κ B-p65-deficient and reconstituted Mefs (Figure 9A) were harvested after washing in cold PBS and collected by centrifugation. The pellet was directly lysed in cell lysis buffer (50 mM HEPES pH 7.4, 50 mM NaCl, 1% Tween20, 2.5 mM EGTA, 1 mM EDTA, 1 mM NaF, 10 mM β -glycerophosphate, 0.1 mM Na₃VO₄, 1 mM PMSF, 1 mM DTT, 1 \times protease inhibitor cocktail from Roche) and incubated for 20 min on ice. The DNA was sheared by three sonication steps of 20 s, and, after ultracentrifugation for 20 min at 100.000g at 4°C, the lysates were further used for western blotting.

For preparation of nuclear protein extracts (Supplementary Figure S4), cells were harvested after washing in cold PBS and collected by centrifugation. The pellet was suspended in extraction buffer A (10 mM HEPES pH 7.9, 10 mM KCl, 1.5 mM MgCl₂, 300 μ M Na₃VO₄, 20 mM β -glycerophosphate, 10 μ M E64, 5 mM DTT, 2.5 μ g/ml leupeptin, 1 μ M pepstatin, 300 μ M PMSF, 1 μ M microcystin), centrifuged (5 min, 2000 r.p.m., 4°C) and resuspended again in extraction buffer A containing NP-40 with a final concentration of 0.1%. After incubation on ice for 10 min, samples were centrifuged (5 min, 13 000 r.p.m., 4°C), and the supernatants (corresponding to cytoplasmic extracts) were collected. Nuclear extracts were prepared by resuspending pellets in extraction buffer B (20 mM HEPES pH 7.9, 420 mM NaCl, 1.5 mM MgCl₂, 200 μ M EDTA, 300 μ M Na₃VO₄, 20 mM β -glycerophosphate, 10 μ M E64, 5 mM DTT, 2.5 μ g/ml leupeptin, 1 μ M pepstatin, 300 μ M PMSF, 1 μ M microcystin, 25% glycerol) followed by mixing, incubation on ice for 30 min and centrifugation (5 min, 13 000 r.p.m., 4°C). The supernatants correspond to nuclear extracts.

Cytosolic and soluble nuclear fractions were prepared as described (43) with the following modifications. Cells were washed twice with ice-cold PBS and harvested by centrifugation (500g, 5 min, 4°C). For separation of soluble and insoluble nuclear fractions (Figure 6B),

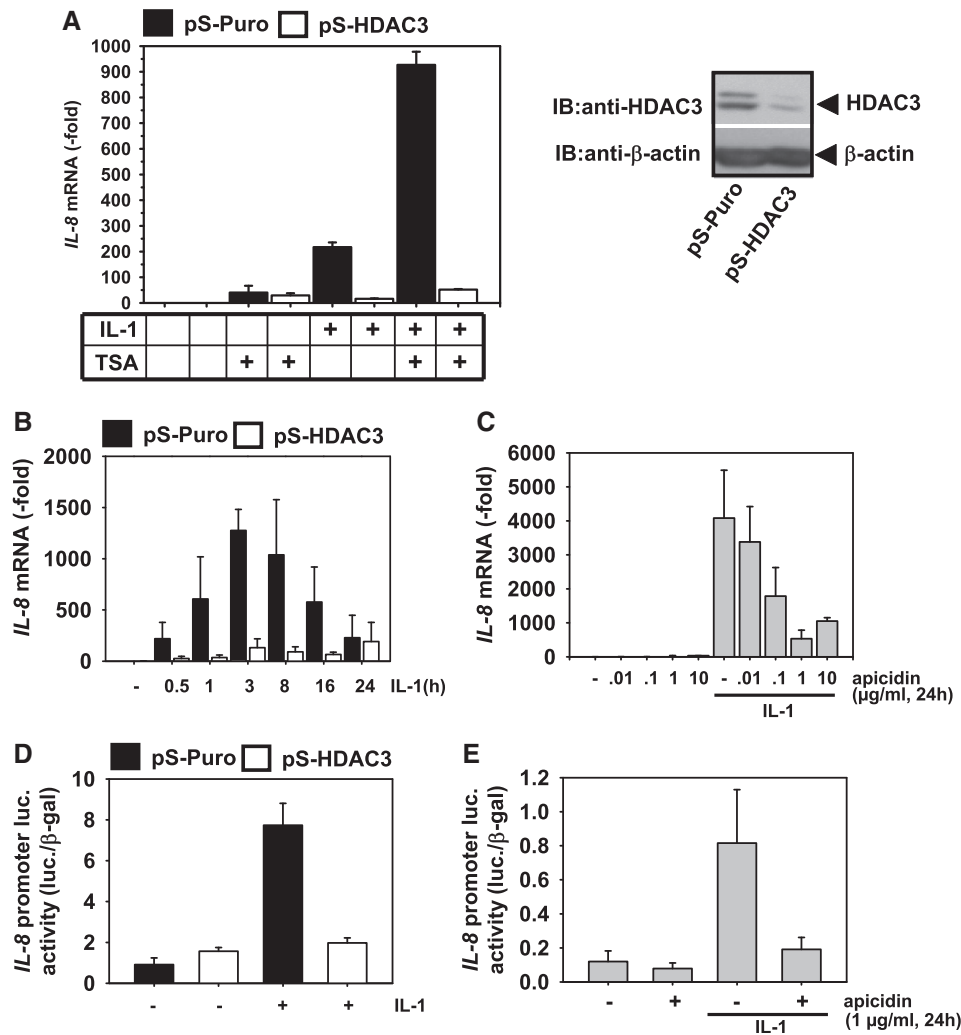


Figure 1. Interference with HDAC3 inhibits *IL-8* transcription. (A) HEK293IL-1R cells were stably transfected with an empty shRNA vector (pS-Puro, black bars) or with a plasmid encoding a HDAC3-specific shRNA (pS-HDAC3, white bars) to generate shRNA-mediated HDAC3 knockdown cells. HDAC3 knockdown and control cells were treated for 3 h with IL-1 (10 ng/ml) or/and for 24 h with TSA (300 ng/ml) as indicated. *IL-8* mRNA expression was determined by RT-qPCR. Data represent the mean *IL-8* expression \pm standard errors of the means (SEM) relative to the unstimulated control ($n = 2$). Black bars: pS-Puro, white bars: pS-HDAC3. The right part shows a control of the knockdown efficiency. Cell lysates were tested by immunoblotting (IB) for the occurrence of HDAC3 and β -actin as a loading control. (B) HDAC3 knockdown (pS-HDAC3, white bars) and control cells (pS-Puro, black bars) were stimulated for the indicated periods with IL-1 and analyzed for *IL-8* mRNA expression as described in (A). Data represent the mean *IL-8* expression \pm SEM relative to the unstimulated control ($n = 2$). (C) HEK293IL-1R cells were pretreated for 24 h with increasing concentrations of the HDAC3 inhibitor apicidin and stimulated for 3 h with IL-1 as shown. RT-qPCR was used to determine *IL-8* mRNA expression, bars show the mean *IL-8* expression \pm SEM relative to the unstimulated control ($n = 2$). (D) HDAC3 knockdown (pS-HDAC3, white bars) and control cells (pS-Puro, black bars) were transiently transfected with an *IL-8* promoter controlled luciferase reporter gene and SV40- β -gal for normalization. Twenty-four hours later, cells were stimulated for 4 h with IL-1 or were left untreated as indicated. Thereafter, cells were lysed, and luciferase and β -galactosidase activities were determined in cell extracts. Shown are the normalized mean luciferase activities \pm SEM from four independent experiments. (E) HEK293IL-1R cells were transiently transfected with an *IL-8* promoter controlled luciferase reporter gene as in (D). Twenty-four hours later, cells were treated for 24 h with 1 μ g/ml apicidin and thereafter stimulated for 3 h with IL-1 or were left untreated as indicated. Thereafter, cell extracts were prepared, and luciferase and β -galactosidase activities were determined. Shown are the normalized mean luciferase activities \pm SEM from two independent experiments.

cells were lysed in lysis buffer 1 (20 mM HEPES pH 8.0, 10 mM KCl, 1 mM MgCl₂, 0.1% Triton X-100, 20% glycerol, 50 mM NaF, 1xRoche protease inhibitor mix, 1 μ M microcystin, 1 mM Na₃VO₄) for 10 min on ice and centrifuged for 1 min at 2300g at 4°C. The supernatant (C, cytosol) was removed, and the pellet was lysed in lysis buffer 2 (20 mM HEPES pH 8.0, 2 mM EDTA, 400 mM NaCl, 0.1% Triton X-100, 20% Glycerol, 50 mM NaF, 1xRoche protease inhibitor mix, 1 μ M

microcystin, 1 mM Na₃VO₄) for 20 min on ice, vortexed twice and centrifuged at 20 400g at 4°C for 5 min. The supernatant (N1, soluble nuclear fraction) was removed, and the pellet was lysed in buffer 3 (20 mM Tris (pH 7.5), 2 mM EDTA, 150 mM NaCl, 1% SDS, 1% NP-40, 50 mM NaF, 1xRoche protease inhibitor mix, 1 μ M microcystin, 1 mM Na₃VO₄). The DNA was sheared by sonication for 20 s, and lysates were incubated for 50 min on ice, repeatedly vortexed and centrifuged at 20 400g at

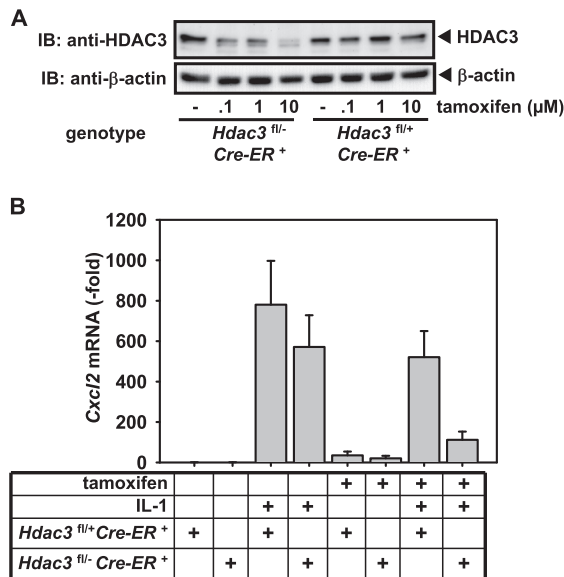


Figure 2. Deletion of the HDAC3 genes inhibits IL-1-triggered *Cxcl2* transcription. (A) Immortalized murine embryonic fibroblast (Mef) lines were generated from mice harboring floxed *Hdac3* alleles and the tamoxifen-inducible *Cre* recombinase gene (33). These cells contain a heterozygous floxed *Hdac3* allele in the wild-type background (*Hdac3^{fl/fl+}*) or in the knockout background (*Hdac3^{fl/fl-}*) and become thus heterozygous for *Hdac3* or lack both *Hdac3* alleles after *Cre*-mediated deletion of the floxed gene. These cells were treated for 72 h with increasing concentrations of tamoxifen as shown and analyzed for HDAC3 and β-actin expression by immunoblotting. (B) The cells with the indicated genotypes were treated for 3 days with 10 μM of tamoxifen and then stimulated for 0.5 h with IL-1 as shown. RT-qPCR was used to quantify *Cxcl2* mRNA expression. Shown are the mean -fold changes compared with the untreated *Hdac3^{fl/fl+}* control line, error bars represent SEM from three different experiments performed in duplicates.

4°C for 5 min. The supernatant (N2, insoluble nuclear fraction) was collected.

Immunoblotting

After electrophoresis on a denaturing polyacrylamide gel, proteins were transferred to a polyvinylidene difluoride membrane (Roth) by semi-dry blotting. After blocking with 5% bovine serum albumin or 5% dried milk in Tris-buffered saline/0.05% Tween for 1 h, proteins were visualized by sequential incubation with primary antibodies for 12–24 h, washed in Tris-buffered saline/0.05% Tween and incubated for 1 h with the peroxidase-coupled secondary antibody. Proteins were detected by using enhanced chemiluminescence systems from Pierce, Millipore or GE Healthcare.

Analysis of p65 acetylation by Ni²⁺-NTA purification

Denaturing purification of p65 was used to visualize p65 acetylation (Figures 4A and 5A, Supplementary Figures S8 and S9), which is readily lost in standard buffers. Cells were harvested, and the washed cell pellet was lysed in 1 ml of lysis buffer A (6 M guanidine-HCl, 0.1 M Na₂HPO₄/NaH₂PO₄, 10 mM imidazole, pH 8.0). The DNA was sheared by one sonication step of 30 s, and lysates were

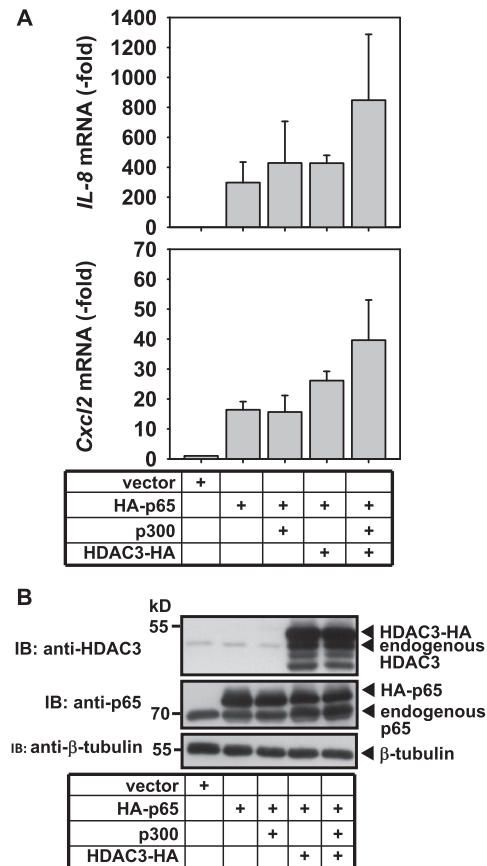


Figure 3. Overexpression of HDAC3 enhances mRNA expression of inflammatory genes. (A) HEK293IL-1R cells were transiently transfected to express wild-type HA-tagged p65 along with p300 and HA-tagged HDAC3. Twenty-four hours later, cells were lysed, and mRNA expression of *IL-8* and *CXCL2* was determined by RT-qPCR. Shown is the mean -fold increase ± SEM relative to the vector-transfected control from two independent experiments. (B) In parallel, expression of HA-tagged p65 and HDAC3 was analyzed by immunoblotting of lysates. One representative out of two experiments is shown. The position of a molecular weight marker is indicated at the left.

cleared by centrifugation for 15 min at 15000g. Also, 1.5 mg of lysate proteins were incubated with 50 μl of Ni²⁺-NTA agarose for 2 h at room temperature on a rotating device. Beads were collected by centrifugation (1 min at 13000g), washed twice in lysis buffer A, twice in a buffer containing 1 volume of lysis buffer A and three volumes of buffer TI (25 mM Tris, 20 mM imidazole, pH 6.8), and twice with buffer TI alone. Bound proteins were eluted by boiling for 10 min at 95°C in 150 μl 1× Roti-Load (Roth). Also, 200 μg of proteins from the initial lysate (input) were precipitated by adding one volume of trichloroacetic acid (TCA) (11%) at 4°C. The pellet was collected at 15000g for 15 min at 4°C, washed once with 200 μl ethanol (100%) (15000g for 15 min at 4°C), air dried and resuspended in 150 μl of 1× Roti-Load (Roth) at 95°C for 10 min. Bound and input protein samples were separated by 7.5% SDS-PAGE including 4.5% glycerol and analyzed by western blotting.

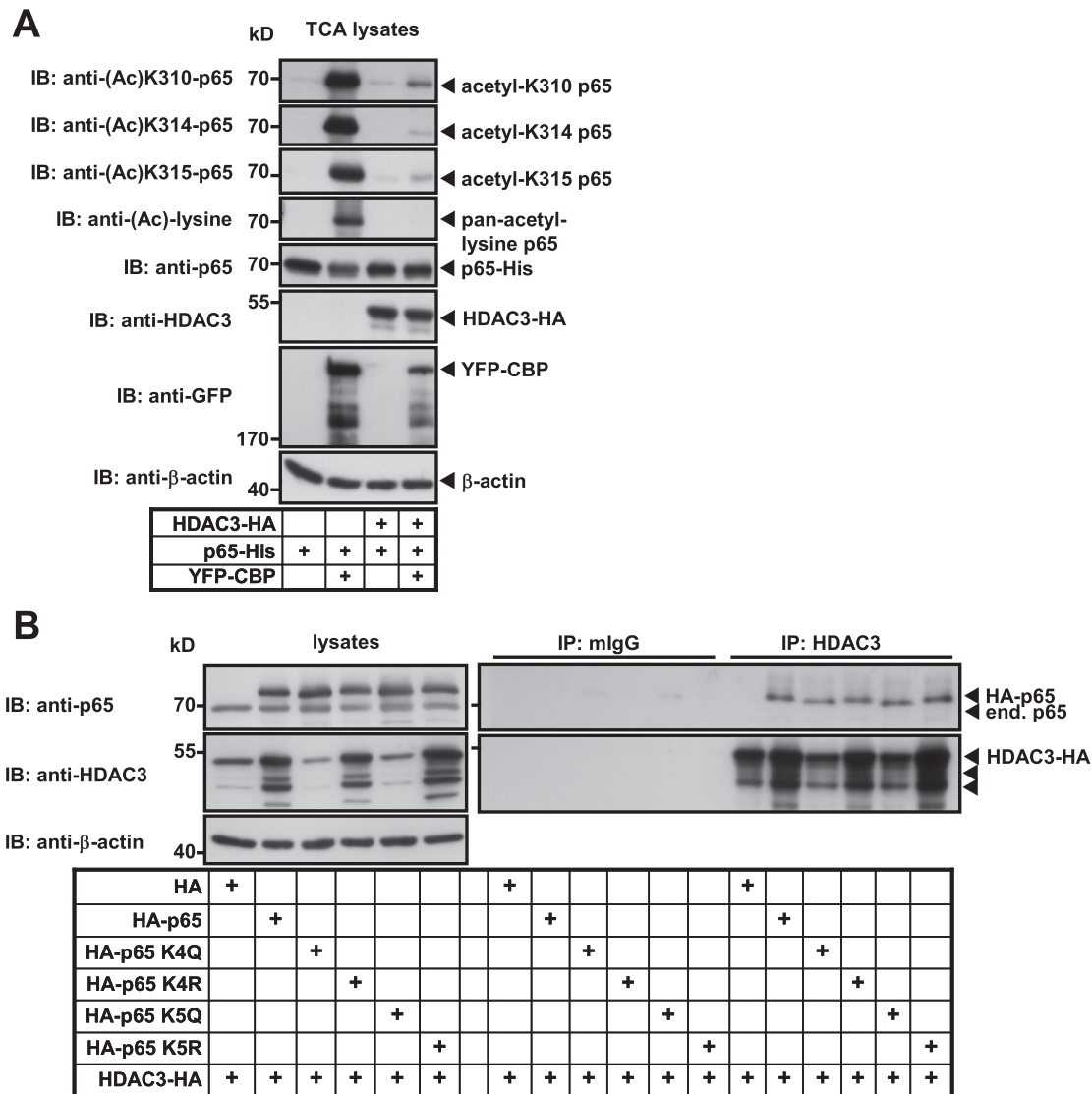


Figure 4. HDAC3 binds to and deacetylates p65 at lysines K310, K314 and K315. (A) HEK293IL-1R cells were transiently transfected to express wild-type His-tagged p65 along with YFP-tagged CBP and HA-tagged HDAC3. Cells were lysed under denaturing conditions, proteins were precipitated by TCA, redissolved and equal amounts were analyzed for general acetylation of p65 with a pan-acetyl-lysine-specific antibody or with antibodies specific for acetylated p65 K310, K314 and K315 as shown. Expression of HDAC3 and YFP-CBP was validated as indicated and equal loading of lanes was confirmed by anti- β -actin antibodies. The position of a molecular weight marker is indicated at the Left (B) HEK293IL-1R cells were transfected to express the indicated combinations of HA-tagged HDAC3 and HA-tagged p65 variants. Following lysis of cells, extracts were used for immunoprecipitation (IP) of the HDAC3 protein, and co-precipitating proteins were revealed with antibodies recognizing p65 NF- κ B. IPs with murine (m) IgG were performed in parallel to control the specificity of the interactions. Arrows mark different HDAC3 isoforms.

Microarray-based mRNA expression analysis and bioinformatic analyses

Human or murine cell lines were transfected and treated as specified in the text. Total RNA was extracted using the Nucleo Spin RNA II-Kit from Macherey & Nagel. The 'Whole Human Genome Oligo Microarray' (G4112F, ID 014850, Agilent Technologies) used for the experiments shown in Figures 7 and 8 contains 45 015 oligonucleotide probes covering the entire human transcriptome. Human samples were processed and finally hybridized according to the two-color mode. The 'Whole Mouse Genome Oligo Microarray V2' (G4846A, ID

026655, Agilent Technologies; Santa Clara, California, USA) used in Figure 9C and Supplementary Figures S6, S7, S11 contains 44 397 oligonucleotide probes covering the entire murine transcriptome. Murine samples were processed and hybridized in single-color mode. Synthesis of Cy3- or Cy5-labeled cRNA was performed with the 'Quick Amp Labeling kit, two color' (#5190-0444, Agilent Technologies) or one color' (#5190-0442), according to the manufacturer's recommendations. cRNA fragmentation, hybridization and washing steps were also carried out exactly as recommended in 'Two-Color Microarray-Based Gene Expression Analysis Protocol V5.7' (see <http://www.agilent.com> for details), except

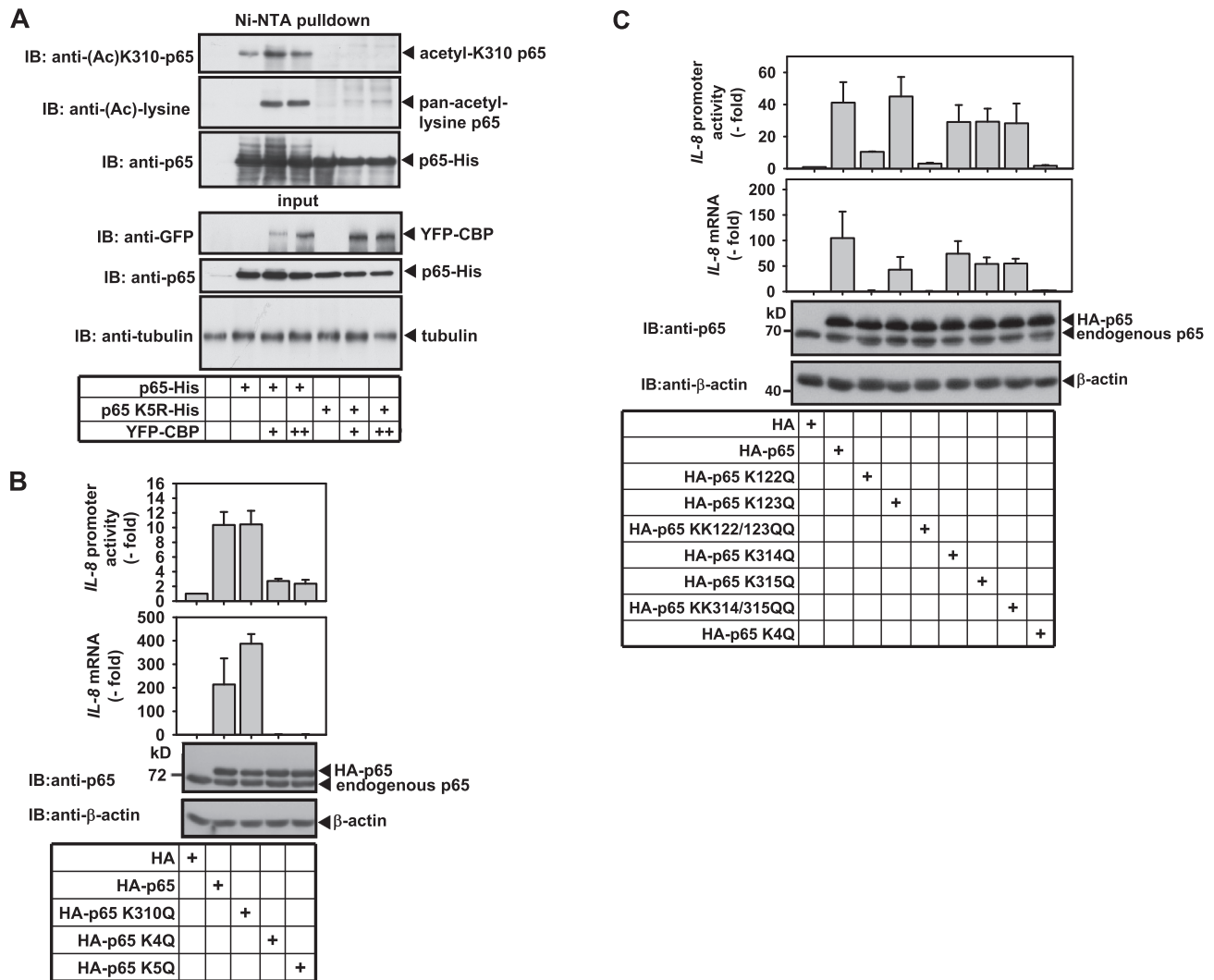


Figure 5. Acetylation mimicking mutants of p65 suppress *IL-8* gene expression. (A) HEK293T cells were transfected with expression plasmids encoding His-tagged p65 wild-type or a mutated version thereof where K122, K123, K310, K314 and K315 (K5R) were mutated to arginines along with 0.75 and 1.5 μ g of a plasmid for YFP-tagged CBP. One fraction of cells was lysed under denaturing conditions to analyze acetylation of p65 with the indicated acetyl-lysine-specific antibodies. The lower part shows the input control ensuring adequate protein expression. (B) HEK293IL-1R cells were transfected with the indicated p65 wild-type and acetylation-deficient expression vectors plus the *IL-8* promoter reporter gene construct and the pSV40- β -galactosidase construct. Twenty-four hours later, cells were lysed, and luciferase reporter gene activity was determined and normalized for β -galactosidase activity. Normalized mean luciferase activities \pm SEM relative to the vector control from five independent experiments (upper graph) are shown. In parallel transfections, cells were transfected to express HA-tagged p65 wild-type or the indicated acetylation-mimicking mutants thereof. The next day, cells were lysed, and one portion of the lysates was analyzed for mRNA expression of the endogenous *IL-8* gene by RT-qPCR. Bars show mean \pm SEM from two independent experiments (lower graph). Another portion was tested by immunoblotting for correct expression of p65. The positions of a molecular weight marker are shown, and the HA-p65 migrates slightly slower than the endogenous p65. (C) HEK293IL-1R cells were transfected with additional p65 mutants and analyzed exactly as described in (B). *IL-8* promoter activity represents the mean \pm SEM from three independent experiments normalized for protein concentration (upper graph). *IL-8* mRNA expression represents the mean fold change \pm SEM relative to the vector control from three independent experiments (lower graph). All samples were analyzed for comparable expression of the constructs in parallel, one representative immunoblot is shown.

that 3–4 μ g of each labeled cRNA sample were used for hybridization. Slides were scanned on the Agilent Micro Array Scanner G2565CA (pixel resolution 5 μ m, bit depth 20). Data extraction was performed with the ‘Feature Extraction Software V10.7.3.1’ by using the recommended default extraction protocol files GE2_107_Sep09.xml (two-color) or GE1_107_Sep09.xml (one-color), respectively.

Data normalization

Microarray raw data extracted by the Feature Extraction software were normalized and analyzed in Genespring GX software, version 11.5.1 (Agilent Technologies). Expression values were log₂ transformed, normalized to 75th percentile of each array and inter array median centered according to the standard procedure in Genespring GX.

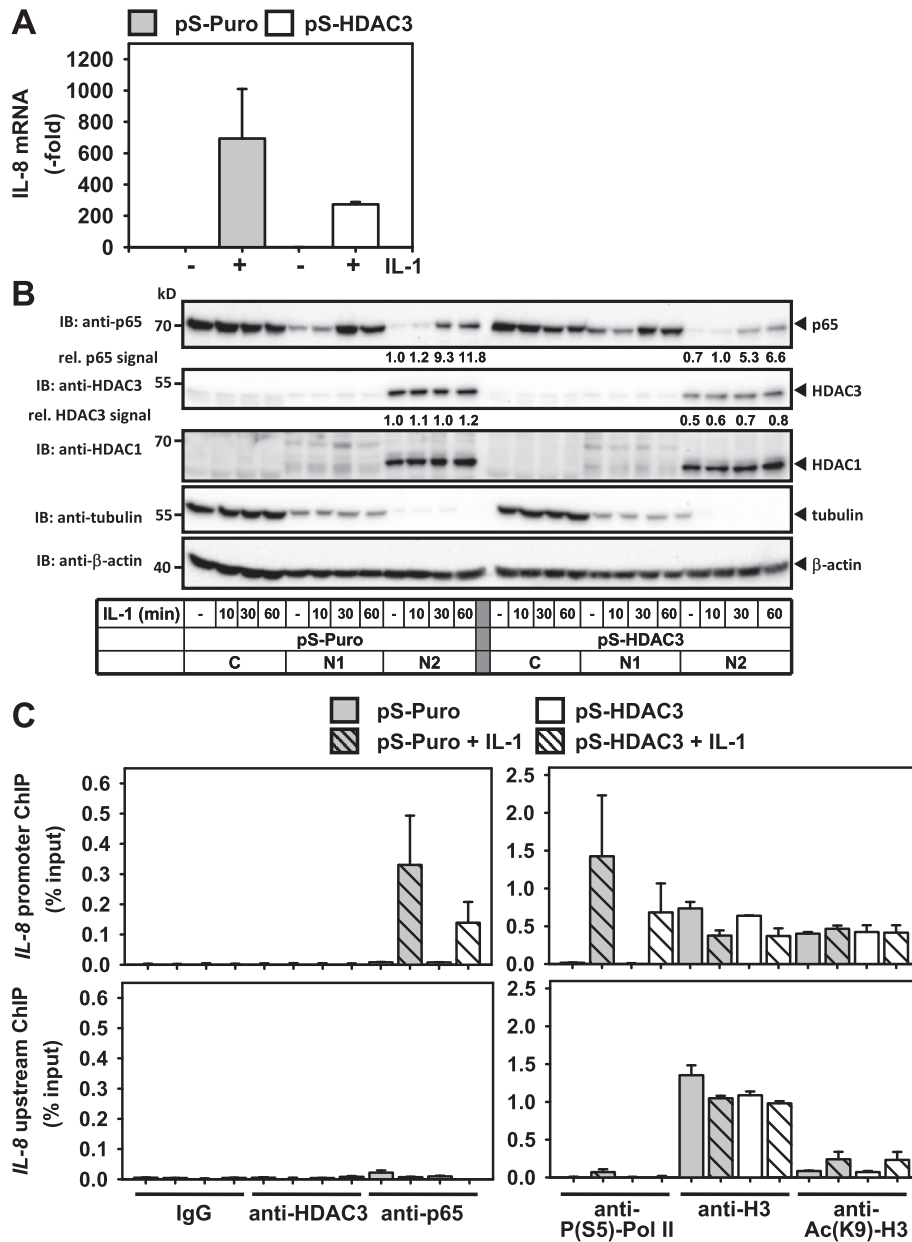


Figure 6. Suppression of HDAC3 affects p65 recruitment and phosphorylation of RNA polymerase II at the *IL-8* promoter. (A) Human KB cells were stably transfected with an empty shRNA vector (pS-Puro, gray bars) or with a plasmid encoding a HDAC3-specific shRNA (pS-HDAC3, white bars) to generate shRNA-mediated HDAC3 knockdown cells. HDAC3 knockdown and control cells were treated for 1 h with IL-1 or were left untreated. *IL-8* mRNA expression was determined by RT-qPCR. Data represent the mean *IL-8* expression \pm SEM relative to the unstimulated control ($n = 2$). (B) The same cells as in (A) were stimulated for the indicated times with IL-1 or were left untreated. Cytosolic (C), soluble nuclear (N1) and insoluble nuclear (N2) extracts were prepared and analyzed for the presence of the indicated proteins by immunoblotting. The amounts of p65 and HDAC3 in the nuclear fractions were quantitated, and expression levels are shown relative to those of untreated cells. Shown is one out of two experiments. (C) The same cells as in (A) were stimulated for 1 h with IL-1 or were left untreated. Chromatin immunoprecipitation was performed using the indicated antibodies and immunoprecipitated DNA was quantified by qPCR using primers spanning the *IL-8* promoter/enhancer region and a non-regulatory upstream region as a negative control. Relative enrichment of immunoprecipitated DNA is shown as percentage of input DNA. Shown are mean values \pm SEM from two independent experiments performed in duplicates.

Identification of TSA- and IL-1-regulated genes in HDAC3 knockdown cells

In all, 29 421 probes with EntrezGeneID showed hybridization signals more than the 20% percentile. Of these, 24 755 probes corresponding to 16 412 genes were measurable in at least 4 of the 16 microarray hybridizations.

This data set was used for further analyses (Figures 7 and 8). The pS-Puro and pS-HDAC3 data sets were filtered separately for genes showing differential regulation by IL-1 by at least 1.5-fold, revealing a total of 75 probes corresponding to 70 genes with consistent regulation. Expression values for these genes above background had to be measurable in at least the stimulated condition (for

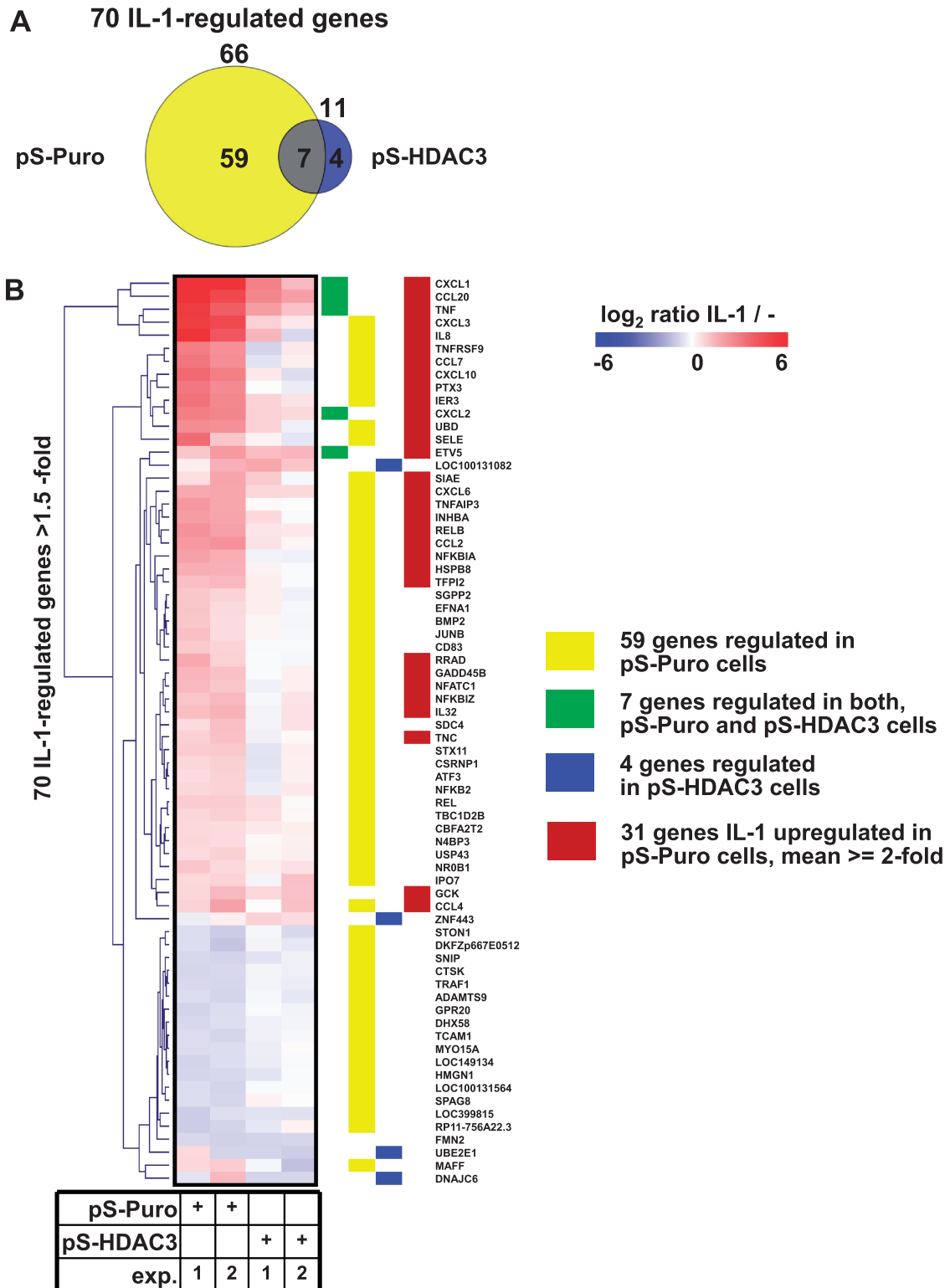


Figure 7. HDAC3 is a global regulator of the transcriptional IL-1 response. HEK293IL-1 R cells stably transfected with pSuper-Puro (pS-Puro) or with pSuper-Puro encoding a shRNA-directed against HDAC3 (pS-HDAC3), as shown in Figure 1A, were treated for 24h with vehicle (EtOH, 0.03%) or with TSA (300 ng/ml). These cells remained unstimulated or were treated for 3h with IL-1. Total RNA was isolated from two independent experimental groups (exp. 1 and exp. 2), labeled cRNA was prepared and was hybridized to whole genome Agilent microarrays. (A) Normalized fluorescence intensity values were used to calculate the total number of genes, which were regulated in the same direction by IL-1 by at least 1.5-fold in both independent experiments compared with the EtOH-treated vehicle control. Data analysis revealed 70 IL-1 regulated genes. Of those, only seven genes are still inducible in the absence of HDAC3, as illustrated by the depicted Venn diagram. (B) The gene set identified in (A) was clustered hierarchically, and ratio values are shown as a colored heatmap. Vertical color-coded bars indicate groups of genes contained in the Venn diagram shown in (A). Brown vertical bars indicate all genes with at least 2-fold regulation by IL-1. The entire data set is shown in Supplementary Table S2.

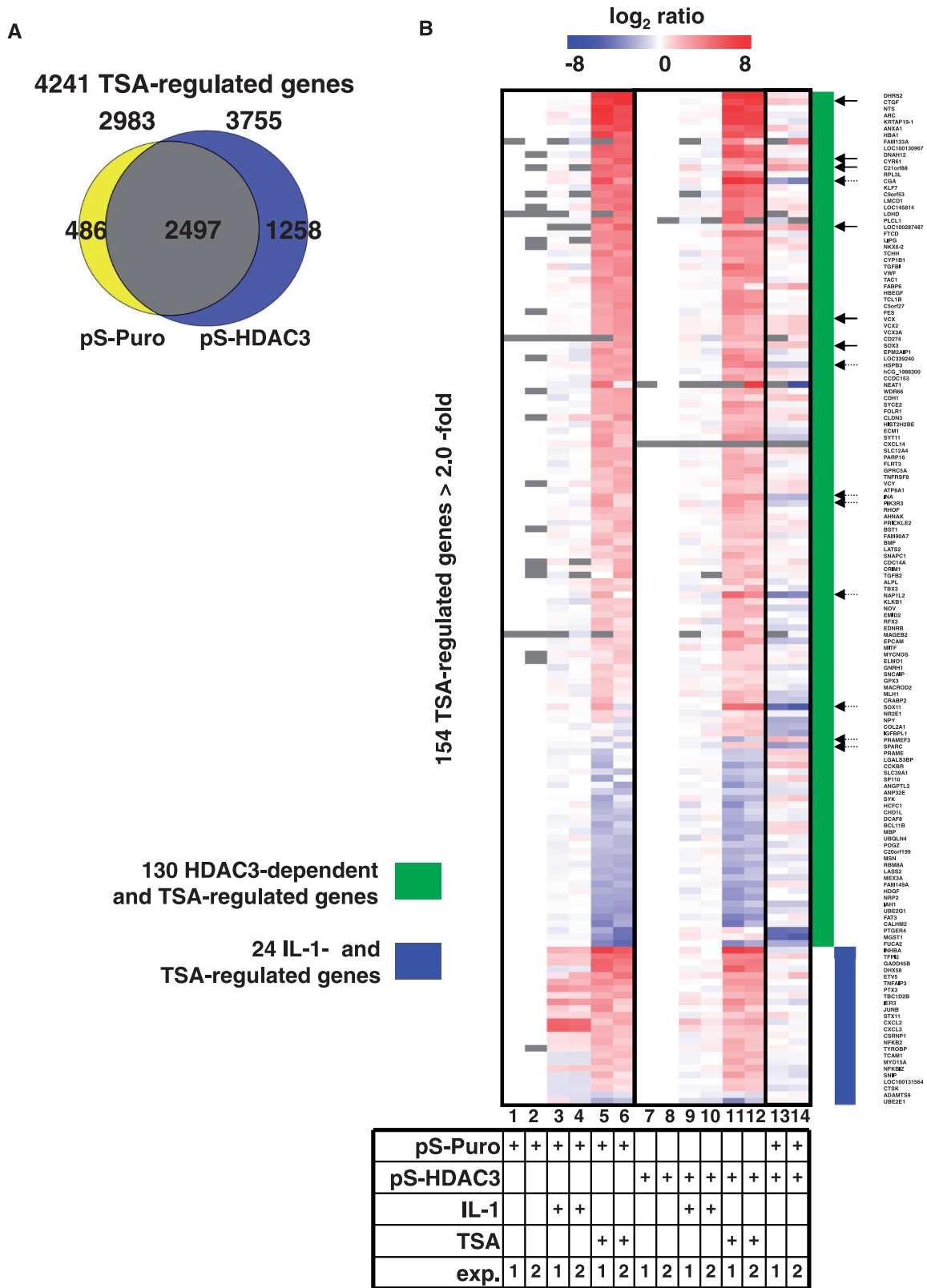


Figure 8. Comparison with the pan-HDAC inhibitor TSA reveals differential and restricted effects of HDAC3 and IL-1 on specific sets of genes. (A) The microarray data set from the experiments described in Figure 7 was used to calculate the total number of genes, which were regulated in the same direction by TSA by at least 2-fold in both independent experiments compared with the EtOH-treated vehicle control. This revealed 4241 genes whose overlap between control cells and HDAC3 knockdown cells is illustrated by the depicted Venn diagram. (B) The TSA-regulated set of genes identified in (A) was additionally filtered for HDAC3-dependent genes based on a ratio of pS-HDAC3/pS-Puro (lanes 13, 14) of at least 1.5-fold in two independent experiments revealing 130 genes. Similarly, the set was filtered for genes, which were regulated by IL-1 by at least 1.5-fold revealing 24 genes. Depicted are color-coded ratio values of all 154 genes, which were calculated by dividing fluorescence intensity measurements of

(continued)

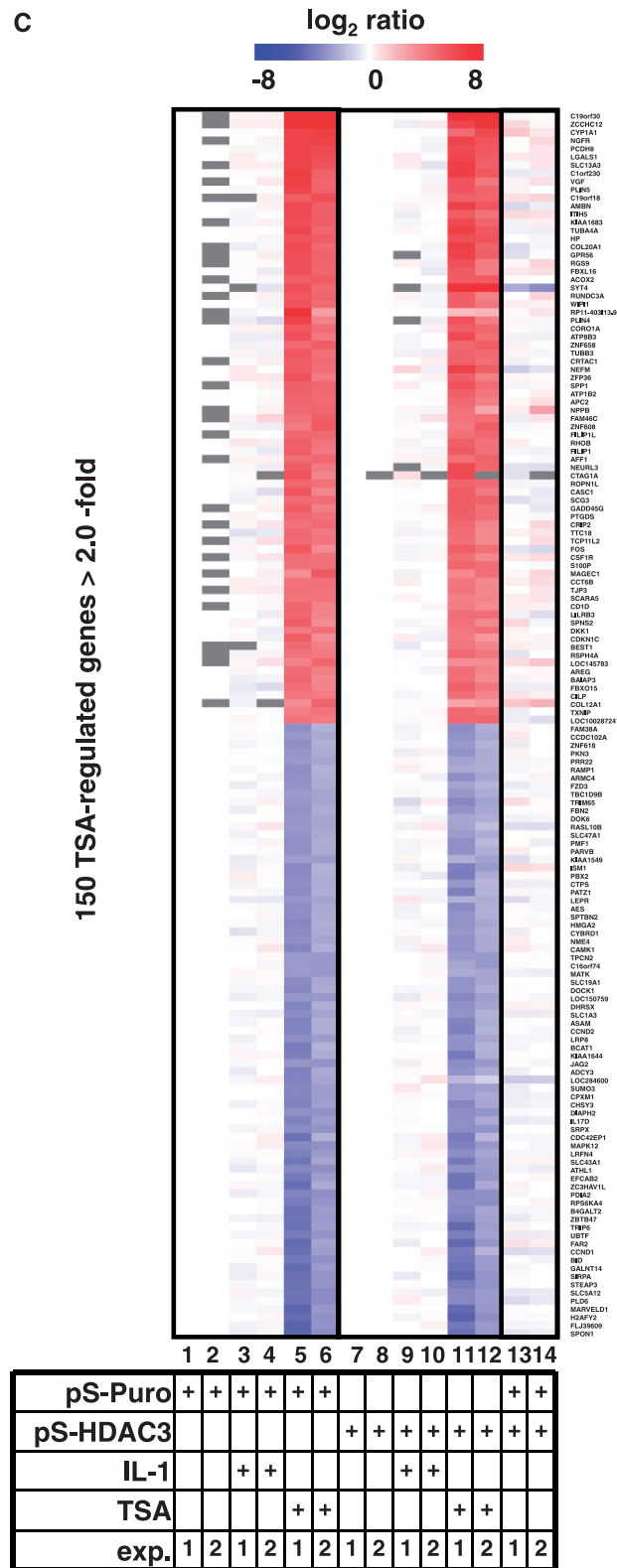


Figure 8. Continued. vehicle-treated cells or IL-1 or TSA treatments by those obtained for the vehicle control situation of either control cells (lanes 1, 2) or HDAC3 knockdown cells (lanes 7, 8). In lane 13 and 14, ratios were calculated by dividing pS-HDAC3 by pS-Puro values. Both data were sorted according to the mean regulation by TSA in descending order. Vertical green and blue bars indicate HDAC3- and IL-1-dependent genes as described for (A). The ratio values from both independent experiments are shown side by side (exp. 1, 2). Solid black arrows indicate examples of genes, which are elevated by both, TSA and HDAC3 knockdown, whereas dotted black arrows indicate genes with adverse regulation by TSA or HDAC3 knockdown, respectively. (C) Depicted are the color-coded ratio values for the 75 most strongly upregulated genes (red colors) or 75 most strongly downregulated genes (blue colors) in response to TSA from the same data set.

upregulated genes) or in the unstimulated condition (for downregulated genes). Differential expression of genes in this final set was significant ($P \leq 0.01$) in at least one out of four comparisons according to feature extraction software algorithms.

In all, 5045 probes showed differential hybridization signals of at least 2-fold in TSA stimulated pS-Puro or pS-HDAC3 cells. This data set was filtered for consistent regulation resulting in 4241 genes: The probes were separated into three subsets: (i) TSA-regulated, HDAC3 knockdown dependent, not IL-1-regulated; (ii) TSA-regulated, HDAC3 knockdown independent, IL-1-regulated; and (iii) TSA-regulated, HDAC3 knockdown independent, not IL-1-regulated. In case of multiple probes per gene in the same subset, only one probe was selected for further analysis. Probe values were removed from other subsets, if probe values for the same gene occurred in intersections of data sets (i–iii). Probes measuring identical genes but having been assigned to different subsets were removed from the data sets.

Identification of IL-1-regulated genes in HDAC3-deficient cells

In all, 25 415 probes with EntrezGeneID corresponding to 15 766 annotated transcripts showed hybridization signals more than the 20% percentile, no flags and were measurable in at least four out of eight microarray hybridizations (Supplementary Figure S6). This data set was filtered for genes showing differential regulation by IL-1 by at least 1.5-fold, revealing a total of 112 probes corresponding to 95 genes with consistent regulation. In all, 593 probes corresponding to 490 genes were regulated by tamoxifen treatment by at least 2-fold in both experiments. Seven of these genes (1.4%) were also regulated by IL-1.

Identification of p65 K4Q- or p65 K5Q-dependent genes

In all, 19 850 probes with EntrezGeneID corresponding to 14 761 annotated transcripts showed normalized hybridization signals more than the 20% percentile and were measurable in at least 8 out of 24 hybridizations (Figure 9C and D and Supplementary Figure S7). This set of data was filtered for genes showing consistent 2-fold regulation in both experiments based on the ratio p65 wild-type/p65^{-/-} (416 probes, 341 genes) or IL-1 + p65 wild-type/p65^{-/-} (908 probes, 836 genes). Only unflagged probes and probes with hybridization signals above 2-fold background signals (>110 fluorescence intensity units) in p65 wild-type or p65 wild-type+IL-1 samples in at least one experiment were included to identify an overlapping set of 975 probes corresponding to 851 IL-1-regulated or p65 target genes. These were further filtered to identify 135 K4Q-dependent or 109 K5Q-dependent genes based on 2-fold ratios (K4Q or K5Q/p65 wild type) and p65 K4Q/p65 K4R ≥ 2.0 or p65 K5Q/p65 K5R ≥ 2.0 .

Clustering and graphical visualization of microarray data

Log₂-transformed ratio values were analyzed by hierarchical cluster analysis using MeV MultiExperimentViewer, version 4.6.2, 2011, (www.tm4.org) with cluster settings

‘average linkage’ as linkage method and ‘Manhattan distance’ for distance measure (44).

Statistics and quantification

Mean and standard errors of the means were calculated using Sigma Plot, version 11.0. Bands detected by immunoblotting were quantified using ImageJ (<http://rsbweb.nih.gov/ij/>).

RESULTS

HDAC3 is required for IL-1 triggered expression of the human *IL-8* gene

We previously found that HDAC3 associated with c-Jun and p65 NF- κ B at IL-1-regulated target genes (45). To further unravel a functional role for HDAC3 in cytokine signaling, we established stable HEK293IL-1R cell lines with a partial shRNA-mediated downregulation of HDAC3 (Figure 1A). These cells and vector controls were stimulated with IL-1 either alone or in combination with TSA, a fungal antibiotic, which inhibits class I and II HDACs roughly to the same extent (46,47). Analysis of *IL-8* expression by RT-qPCR showed that IL-1-triggered *IL-8* mRNA was further stimulated by TSA in a synergistic manner (Figure 1A), which is in accordance with the general role of HDACs as negative regulators of acetylation-dependent chromatin relaxation (48). In marked contrast, knockdown of endogenous HDAC3 by shRNA strongly inhibited IL-1-induced *IL-8* expression, indicating an important role of HDAC3 for productive *IL-8* transcription (Figure 1A). To further investigate this finding in a time-resolving manner, control and HDAC3 knockdown cells were stimulated for various periods with IL-1, followed by analysis of *IL-8* mRNA expression by quantitative RT-qPCR (Figure 1B). These experiments revealed a critical role of HDAC3 for gene expression during the induction and peak phases of the *IL-8* response.

As some HDAC3-dependent effects are independent from its enzymatic function as a deacetylase (49), it was then important to measure IL-1-induced *IL-8* transcription in the presence of the inhibitory compound apicidin, which selectively inhibits HDAC3 and also with a minor efficiency HDAC2 (50,51). Increasing concentrations of apicidin blocked induced *IL-8* mRNA expression in a dose-dependent manner in HEK293IL-1R cells (Figure 1C) and also in the tumor cell lines KB and A549 (Supplementary Figure S1), thus revealing the importance of the enzymatic function of HDAC3 for its stimulatory function on transcriptional regulation of gene expression.

As HDACs can regulate gene expression by global effects on chromatin compaction (52), it was interesting to investigate whether HDAC3 inhibition also affects gene expression from an *IL-8* promoter that is not embedded into its native chromatin context. To address this question, HEK293IL-1R cells were transfected with a luciferase plasmid under the control of an *IL-8* promoter. IL-1 triggered luciferase expression was diminished in HDAC3 knockdown cells (Figure 1D) or in the presence of

apicidin (Figure 1E), showing that HDAC3-mediated effects directly control transcriptional activation of the *IL-8* promoter in a chromatin-independent manner.

HDAC3 is required for IL-1 triggered expression of the murine *Cxcl2* gene

To investigate the contribution of HDAC3 on inflammatory gene expression by an independent experimental approach, we performed further experiments with immortalized Mef lines generated from mice harboring floxed *Hdac3* alleles, which were crossed with mice containing a tamoxifen-inducible *Cre* recombinase gene (33). These cells contain a heterozygous-floxed *Hdac3* allele in the wild-type background (*Hdac3^{fl/+}*) or in the knockout background (*Hdac3^{fl/-}*) and thus become heterozygous for *Hdac3* or lack both *Hdac3* alleles after *Cre*-mediated deletion of the floxed gene. To determine the optimal dose of tamoxifen for efficient HDAC3 knockout, cells were treated for 3 days with increasing concentrations of tamoxifen and analyzed for HDAC3 protein levels by immunoblotting. These experiments revealed strong reduction of HDAC3 levels at a concentration of 10 μ M tamoxifen (Figure 2A). Ablation of HDAC3 under these conditions also resulted in reduced cell viability (data not shown), which is in line with its reported necessity for maintenance of genome stability and S phase progression (30,33). To study a role of HDAC3 in this genetically altered system after the induction of gene deletion by tamoxifen, these cells remained untreated or were stimulated by IL-1, followed by analysis of *Cxcl2* transcription by RT-qPCR (Figure 2B). Loss of one *Hdac3* allele slightly reduced IL-1-triggered *Cxcl2* expression, whereas deletion of both alleles strongly impaired the transcriptional response (Figure 2B). Control experiments ensured that these inhibitory effects are not due to any tamoxifen-mediated effects, as in two other Mef lines *Cxcl2* expression was not suppressed but rather weakly induced on tamoxifen treatment (Supplementary Figure S2). Moreover, four shRNA oligonucleotides directed against murine HDAC3 also suppressed IL-1-inducible *Cxcl2* expression (Supplementary Figure S3). Together with the experiments involving human cells (Figure 1 and Supplementary Figure S1), these data provide several independent lines of evidence for a positive role of HDAC3 for IL-1-mediated gene expression.

HDAC3-mediated p65 deacetylation augments NF- κ B transcriptional activity

The pro-transcriptional activity of HDAC3 raises the question for its molecular target(s) that mediate this effect. The expression of *IL-8* (36) and *Cxcl2* (53) depend on NF- κ B and HDAC3 has been reported to interact with NF- κ B p65 (9). Ectopic expression of p65 activated expression of endogenous *IL-8* and *Cxcl2* genes (Figure 3). Moreover, co-expression of HDAC3 enhanced p65-mediated expression of both genes, an effect which was pronounced in the presence of p300 (Figure 3A and B). To identify the molecular basis for this activating effect of HDAC3, we tested whether HDAC3 can lead to the deacetylation of p65. Cells were

transfected to express His-tagged p65 and CBP along with an expression vector for HDAC3 and were lysed under denaturing conditions to prevent removal of acetyl groups after cell lysis, and His-tagged p65 was enriched on Ni-NTA matrices. The acetylation status of p65 was analyzed by immunoblotting with pan-acetyl-lysine-specific antibodies or with three different antibodies recognizing site-specific acetylation at lysines 310, 314 and 315 (Figure 4A). These experiments showed that CBP-induced acetylation of p65 was largely lost in the presence of HDAC3, as revealed by the use of the pan-acetylation antibody and also by the site-specific antibodies recognizing p65 acetylated at lysines 310, 314 or 315. These data revealed HDAC3 as a major and specific p65 deacetylase.

Given the reported interaction between p65 and HDAC3 (9), we designed experiments to analyze the possible regulation of this association. As substrate binding of HATs can be regulated by binding to acetylated lysine moieties via bromodomains (21), we compared binding of HDAC3 between wild-type p65 and mutants thereof, which were changed in four (K122, K123, K314, K315) or all five (K122, K123, K310, K314, K315) known acetylated lysines either in a lysine acetylation inactivating way to arginine (p65 K4R, p65 K5R) or in a lysine acetylation mimicking way to glutamine (p65 K4Q, p65 K5Q). Coimmunoprecipitation experiments confirmed the HDAC3/p65 interaction and showed similar HDAC3 binding of all p65 mutants (Figure 4B). The slightly impaired binding of the p65 K4Q or p65 K5Q mutants is attributable to a lower general expression of HDAC3 in the presence of p65 K4Q or p65 K5Q, which might be due to inhibitory effects on cryptic NF- κ B binding sites in the vector sequences driving the expression of the HDAC3 cDNA. To investigate the role of p65 acetylation in more detail, we generated a p65 mutant that is widely refractory to acetylation. As the p65 K4R mutant still contains the acetylated lysine 310 (10), we used a mutant where also this lysine was mutated to arginine (p65 K5R). Although expression of CBP triggered acetylation of wild-type p65, the p65 K5R mutant was completely devoid of any acetylation (Figure 5A), thus excluding the existence of additional major acetylation sites in p65. This experiment, therefore, revealed the suitability of K5 mutants for further experiments.

In a next step, transcriptional activation mediated by p65 wild-type was compared with that of various p65 K/Q mutants mimicking acetylation at one or several lysines. Cells were transfected to express similar amounts of these different p65 variants (Figure 5B), followed by the analysis of *IL-8* transcription by reporter gene assays (Figure 5B, upper graph) or *IL-8* mRNA expression by RT-qPCR (Figure 5B, lower graph). Although wild-type p65 strongly activated *IL-8* mRNA expression and transcription, the p65 K310Q mutant was slightly more active in activating mRNA expression, which is in line with published data on a positive role of acetylation at K310 for NF- κ B activity (10). In striking contrast, the p65 K4Q and p65 K5Q mutants had lost their transactivating capacity to induce *IL-8* mRNA expression and transcription

(Figure 5B), although *in vitro* their DNA-binding and dimerization capacities are known to be fully intact (15).

To delineate the role of acetylation-mimicking mutations of K122, K123, K314 and K315 in more detail, these residues were mutated individually or in tandem combinations. Analysis of *IL-8* transcription and mRNA expression revealed a strong inhibitory effect of the K122Q mutation, whereas mutations of K123, K314 and K315 were less inhibitory (Figure 5C).

HDAC3 is required for IL-1-induced recruitment of p65 NF- κ B and RNA polymerase II phosphorylation at the *IL-8* promoter

Acetylation of K122 and K123 has been previously implicated in reduction of p65 DNA-binding *in vitro* (9). To assess the effects of HDAC3 knockdown on NF- κ B nuclear translocation, overall DNA-binding and recruitment to the endogenous *IL-8* gene, we used KB cells that we found previously well suited for chromatin immunoprecipitation (ChIP) analysis of IL-1-induced genes (36). Similar to HEK293IL-1R cells, HDAC3 knockdown in KB cells diminished IL-1-induced *IL-8* expression (Figure 6A). To test the impact of HDAC3 on IL-1-triggered translocation of p65 to the nucleus, cells were stimulated with this proinflammatory cytokine and fractionated. Western blot experiments showed that knockdown of HDAC3 did not affect IL-1-induced accumulation of p65 in the soluble nuclear fraction, whereas the amount of p65 in the insoluble nuclear fraction was reduced by 50% (Figure 6B). This result suggests that HDAC3 does not modulate cytosolic pathways mediating p65 nuclear translocation but rather is required for stable association of p65 with chromatin. To investigate this possibility further, ChIP were performed, which showed reduced recruitment of p65 NF- κ B to the *IL-8* promoter (Figure 6C). Further ChIP experiments revealed that downregulation of HDAC3 also resulted in strongly reduced amounts of RNA polymerase II phosphorylated at serine 5 at the *IL-8* promoter, which is in line with its negative effects on *IL-8* mRNA synthesis. Control experiments showed no association of p65 binding and RNA polymerase II phosphorylation at a region 940 bp upstream of the *IL-8* promoter, demonstrating the specificity of the ChIP analyses (Figure 6C). Compared with this upstream region, the *IL-8* promoter displayed a lower density of histone H3 and higher acetylation of histone H3 at lysine 9, which suits the needs for a more open chromatin structure of this rapidly inducible gene (Figure 6C). HDAC3 knockdown cells showed no changes of histone H3 loading and acetylation (Figure 6C) arguing for specific effects of HDAC3 on transcriptional activators of *IL-8* rather than on more general changes of the local chromatin structure. These effects seem to be independent from stable association of HDAC3 with chromatin, as we were not able to detect stable HDAC3 recruitment to the *IL-8* locus by ChIP (Figure 6C) or by ChIP followed by deep sequencing of DNA (ChIP-seq) (data not shown) with the antibodies available to us.

These data indicate that acetylation of at least one residue of lysines 122, 123, 314 and 315 accounts for

inhibition of p65 activity for *IL-8* expression and suggest that removal of these acetyl groups by HDAC3 is a necessary positive regulatory step in the nucleus, which facilitates contact of p65 with specific DNA elements for activating p65-driven gene transcription.

A general role of HDAC3 for the induction of the IL-1-gene response

Previous studies have shown that the effect of NF- κ B p65 modifications occur in a highly gene-specific fashion (15,54). It was therefore interesting to investigate the role of HDAC3 in IL-1-induced gene expression at a genome-wide level. HDAC3 knockdown cells and vector controls were stimulated with IL-1 and compared with cells in which global acetylation was boosted on TSA-mediated inhibition of all major HDACs. Successful TSA treatment was confirmed by TSA-induced histone H3 acetylation (Supplementary Figure S4).

Gene expression was measured by two independent high density microarray experiments, followed by data filtering for genes regulated consistently in the same direction. These experiments allowed the identification of 70 genes regulated by IL-1 by at least 1.5-fold in two independent experiments (Figure 7A). Only seven genes were still inducible in HDAC3 knockdown cells, showing that HDAC3 is required for the majority of all IL-1-induced genes in HEK293IL-1R stable cell lines (Figure 7A).

A hierarchical cluster analysis of the groups of genes identified in Figure 7A visualizes the individual relevance of HDAC3 for virtually all IL-1-inducible genes (Figure 7B, yellow and green bars). These findings were confirmed in a time-resolving fashion by RT-qPCR for the selected target genes *CXCL1*, *CXCL2*, *CXCL3* and *NFKBIA* (Supplementary Figure S5).

To support this conclusion by an independent experimental approach, IL-1-induced gene expression was compared between control Mefs and Mefs treated with tamoxifen to obtain Cre-inducible ablation of the *Hdac3* gene. As shown in Supplementary Figure S6A, we found 95 genes that were induced by IL-1 by at least 1.5-fold in two independent experiments. The expression of 40 of them was suppressed by at least 2-fold after tamoxifen-induced deletion of *Hdac3*. Tamoxifen itself had weak inducing, but no inhibitory, effects on several of these genes (Supplementary Figure S6B). Although 490 genes were regulated at least 2-fold by tamoxifen in both experiments, only seven genes (1.4%) were inducible by IL-1 (Supplementary Figure S6B). In summary, these data show that the broad and co-stimulatory role of HDAC3 for the IL-1-triggered transcriptional program is not restricted to human cells and can also be found in mice.

Comparison with the pan-HDAC inhibitor TSA reveals differential and restricted effects of HDAC3 on specific sets of genes

In addition, we interrogated the entire data set obtained for HEK293IL-R cells for genes whose expression depends on TSA-sensitive HDACs as compared with HDAC3 alone. Because the group of TSA-regulated

genes was very large, we initially used a 2-fold cut-off for identifying 2983 TSA-regulated genes in control cells and 3755 TSA-regulated genes in cells depleted for HDAC3 (Figure 8A). Of those, 2497 genes were regulated by TSA in both cell lines, which correspond to 83.71% of all genes from control cells and 66.5% of all genes from HDAC3 knockdown cells, revealing that transcriptome-wide TSA effects are largely independent from the HDAC3 expression level (Figure 8A). This interpretation was corroborated by visualizing ratios of expression for individual genes (Figure 8B). Using an additional 1.5-fold cut-off, we identified a group of 130 TSA-sensitive genes whose expression was also altered in HDAC3 knockdown cells (Figure 8B, green bar). Of these, 68 were up- and 62 were downregulated constitutively in HDAC3 knockdown cells compared with control cells, indicating that their constitutive expression levels are modulated by HDAC3 (Figure 8B, green bar, lanes 13, 14). Some genes were elevated by both, TSA or HDAC3 knockdown (e.g. *CTGF*, *CYR61*, *C2lorf88*, *LOC100287487*, *VCX*, *SOX3*), suggesting that their repression is under control of HDAC3. Importantly, in several cases, genes were regulated in the opposite direction by TSA treatment or HDAC3 knockdown (e.g. *CGA*, *HSPB3*, *INA*, *PIK3R3*, *NAPI2*, *SOX11*, *PRAMEF3*, *SPARC*), indicating that HDAC3 plays a highly distinct role in their regulation (Figure 8B).

This interpretation is in line with the result that the overall induction or repression pattern of these 130 TSA-regulated genes was almost identical between control and HDCA3 knockdown cells (Figure 8B, green bar, compare lanes 5, 6 with lanes 11, 12) adding further evidence for a highly selective role of HDAC3 in gene expression. Moreover, as shown by the ratio values indicated by the blue vertical bar, we also found 24 TSA-sensitive genes, which were also inducible by IL-1 (Figure 8B, blue bar). Although their expression was suppressed by HDAC3 knockdown (Figure 8B, blue bar, compare lanes 3, 4 with lanes 9, 10), their induction by TSA was independent of HDAC3 (Figure 8B, green bar, compare lanes 5, 6 with lanes 11, 12). Hence, the data shown in Figure 8A and B suggest that only a small fraction of TSA-regulated genes is controlled by HDAC3.

Further support for this interpretation comes from the analysis of the 150 most strongly up- or downregulated TSA-sensitive genes. These highly regulated genes were neither affected by HDAC3 knockdown nor by IL-1 (Figure 8C). Therefore, the top-ranking group of genes regulated by TSA-sensitive HDACs is clearly distinct from the smaller set of genes, which is regulated by IL-1 and HDAC3.

In conclusion, HDAC3 knockdown does not have a general repressive or inducing effect on the transcriptome *per se* and has little effect on global changes of gene expression compared with genome-wide-induced changes of chromatin structure using pharmacological blockade of HDACs. Our data also show that HDAC3 rather serves as a co-activator for the majority of IL-1-induced genes and thus identify it as a IL-1-specific nuclear signal integration node.

Acetylation of p65 down-regulates IL-1-target genes

We then investigated whether the stimulatory effects of HDAC3 on gene expression is associated with its ability to control the acetylation status of p65 NF-κB. P65-deficient Mefs stably reconstituted to express comparable amounts of wild-type, acetylation-deficient (K/R) or acetylation-mimicking p65 (K/Q) (Figure 9A) were

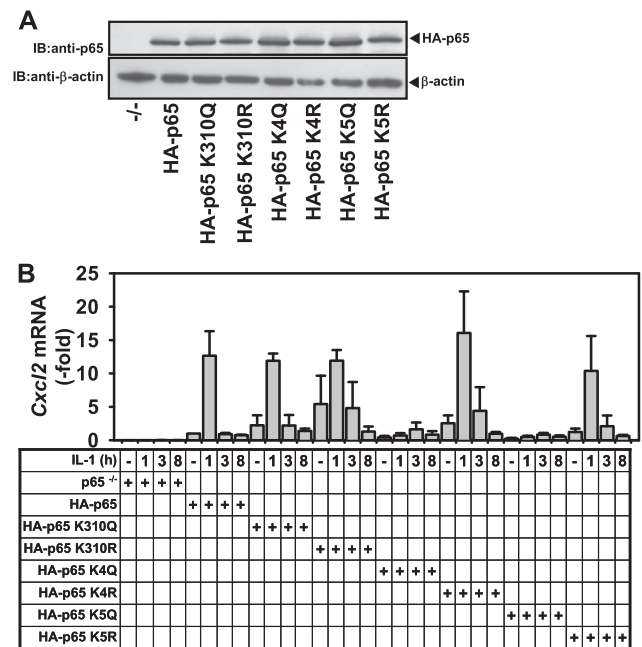


Figure 9. Specific inhibitory effects of p65 NF-κB acetylation-mimicking mutants on IL-1-induced gene expression. (A) NF-κB p65-deficient Mefs (p65^{-/-}) were reconstituted to express p65 NF-κB wild-type (HA-p65) and its mutant forms as described in (15). A representative western blot ensuring expression of comparable amounts of p65 proteins is shown. (B) Mefs were stimulated for various periods with IL-1 as indicated. Expression of *Cxcl2* was analyzed by RT-qPCR. Relative changes of mRNA expression compared with untreated cells reconstituted with p65 NF-κB wild-type were calculated. Shown are the relative mean values ± SEM from three independent experiments compared with cells reconstituted with wild-type p65 (set as 1). (C and D) Two RNA preparations from experiments performed as described in (B) were used to prepare cRNA and to hybridize whole genome Agilent microarrays. A set of 851 p65-dependent or IL-1-induced genes was extracted based on 2-fold regulation in both experiments. This set was further filtered for genes affected by p65 K4Q or p65 K5Q. Color-coded ratio values for the top-ranking genes of these two subsets are shown. The entire sets of data are shown in Supplementary Figure S7A and B. Gray colors indicate genes with low hybridization signals on the microarrays. (C) Expression values were used to identify 851 genes, which were regulated by IL-1 (ratio IL-1 p65 wild-type/p65^{-/-}) or are dependent on p65 NF-κB (ratio p65 wild-type/p65^{-/-}). These genes are sorted according to mean regulation by IL-1 in descending order and are indicated by the green vertical bar. Genes regulated by IL-1 and suppressed by p65 K4Q (blue vertical bars) or by p65 K5Q (brown vertical bars) were identified by ratio values of p65 wild-type+IL-1/p65 K4Q+IL-1 or p65 K5Q+IL-1 ≥ 2.0. (D) Expression values were used to identify 167 genes, which were dependent on p65 NF-κB (ratio p65 wild-type/p65^{-/-}) and regulated by p65 K4Q (yellow vertical bars) or by p65 K5Q (purple vertical bars) based on the ratio p65 K4Q/p65 K5Q/p65 wild-type followed by p65 K4Q/p65 K4R and by p65 K5Q/p65 K5R. These genes are sorted according to mean regulation by p65 K4Q in descending order.

(continued)

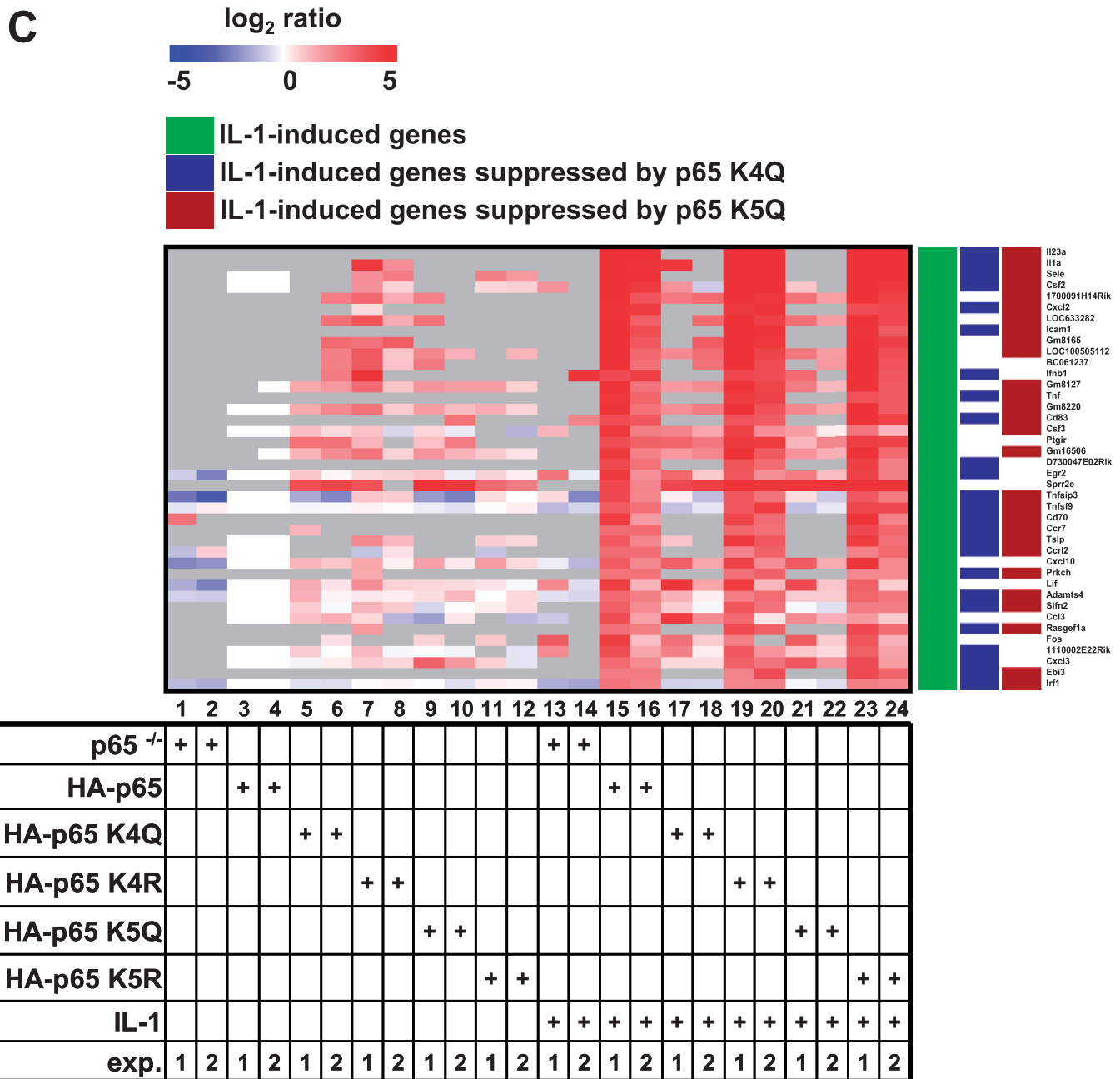


Figure 9. Continued.

stimulated with IL-1 and analyzed for transcription of the endogenous *Cxcl2* gene by RT-qPCR. These results revealed a p65-dependent robust activation of gene expression and slightly elevated basal *Cxcl2* expression in cells expressing acetylation-deficient p65 proteins (Figure 9B). However, the p65 K4Q and K5Q mutants had lost their ability to induce *Cxcl2* expression in response to IL-1 at all time points tested (Figure 9B). In line with the results of transiently transfected human cells (Figure 5), the acetylation-mimicking mutant K310Q was not inhibitory, suggesting that acetylation at, at least, one residue of K122, 123, 314 and 315 is mediating the inhibitory effect (Figure 9B).

We also tested the effects of reconstituted p65 K4Q or p65 K5Q mutants on the entire IL-1 response by performing 24 high density microarrays from two independent series of experiments. We filtered these data sets using 2-fold cut-offs for p65 NF- κ B-dependent and for IL-1-regulated genes. In this group of 851 genes, the majority of IL-1-induced genes was suppressed by the p65 K4Q or K5Q mutants, suggesting that acetylation of p65 is a general negative regulator of inflammatory gene expression programs (Figure 9C). Of note, the K4R and K5R mutants reverted to a large extent the K4Q or K5Q effects arguing that these mutations inactivate the acetylation phenotype (Figure 9C).

D

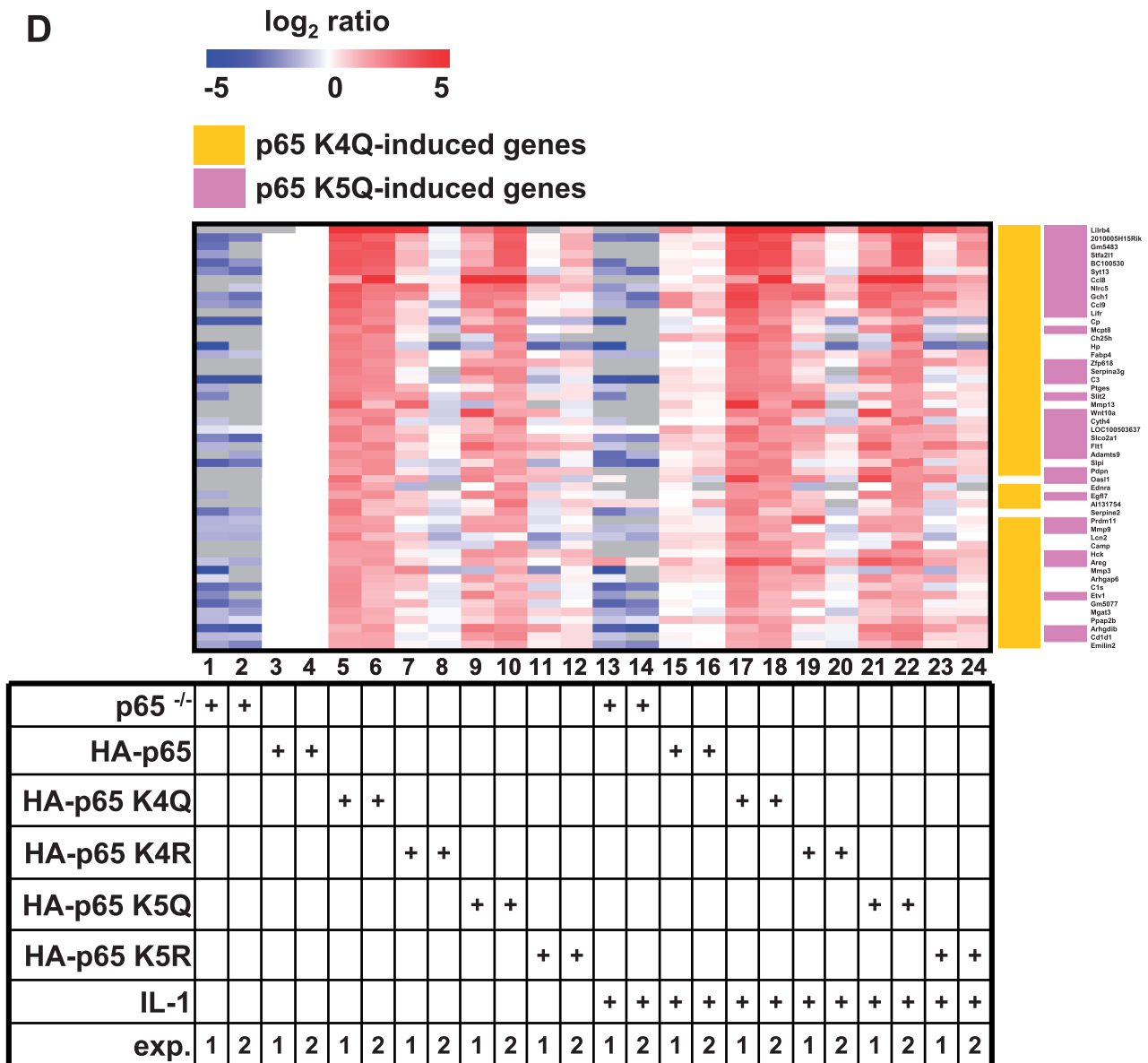


Figure 9. Continued.

We also used the same data set to explore whether the p65 K4Q or K5Q mutants were completely devoid of activating genes. Interestingly, in unstimulated cells, we found that p65 K4Q or p65 K5Q upregulated 77 genes and repressed 56 genes. As shown in Figure 9D and Supplementary Figure S7, a large part of these genes was repressed in p65-deficient cells and re-expressed by reconstituting p65 wild-type, proving that they are *bona fide* p65 target genes. In most cases, K-Q and K-R mutants had opposite effects on gene expression (Figure 9C and D). These data support the conclusion that acetylation-mimicking confers gene-specific properties of p65. Moreover, such mutants had lost their ability to trigger IL-1-dependent gene expression, thus corroborating the concept that inhibitory p65 acetylations need to be relieved by HDAC3 to activate cytokine-responsive genes.

Discussion

In this study, we provide several lines of evidence that besides its well-defined role as catalytic subunit of co-repressor complexes, HDAC3 can also function as a co-activator in inflammatory signaling pathways.

Our data further suggest that a substantial portion of the co-activating property of HDAC3 is mediated by the removal of inhibitory acetyl groups from NF-κB p65, as (i) HDAC3 deacetylates p65 NF-κB at all known lysine residues; (ii) 19 (48%) of 40 HDAC3-dependent IL-1 response genes require p65 for expression (Supplementary Table S1); and (iii) mimicking acetylation of p65 at these sites results in p65 variants with strongly diminished gene-activating properties for inflammatory genes. The p65 5KQ mutant is not generally

transcriptionally inactive, as a recently published gene array analysis in reconstituted and TNF-stimulated cells showed that p65 5KQ was able to induce the TNF-stimulated genes *Ccl9* and *Mmp9* at levels comparable with the wild-type p65 protein (15). Here, we extended this analysis and found a larger group of genes whose constitutive p65 NF- κ B-dependent expression was enhanced by either the K4Q or the K5Q mutant (Figure 9). These data exclude non-specific and general functional defects for the p65 K-Q mutants and underscore their suitability as gain-of-function mutants mimicking p65 acetylations. Of note, data acquired with the p65 K/R mutants are more difficult to interpret, as they reflect defective acetylation and strongly impaired ubiquitination (15). This also relates to findings on the role of K122 and K123, which have been previously implicated in a mechanism involving I κ B-mediated removal of p65 from the IL-8 promoter on the basis of KK122/123/RR mutations (9). These mutations may either affect p65:chromatin interactions or alter degradation of promoter bound p65 (55). This may also explain why so far the functional exploration of p65 acetylation (which thus far has only been addressed by the use of K/R mutants) has not revealed a coherent picture (5,7,8,12). Thus, the data provided in this study using K-Q mutations provide novel evidence for specific gene-regulatory functions of p65 acetylations.

Research on p65 acetylation has also been limited, as primarily, the acetylation site K310 was investigated owing to the availability of a specific antibody (10,11,16,56). Here, using two other specific antibodies developed by us (12,14), we show that modifications at K314 and K315 play a different role. Like for K310, acetylation at these sites is removed by HDAC3. But in contrast to acetylation of K310, which activates transcription of the *cIAP-2* gene (57), we show here by means of the K4Q mutant and by individual K-Q mutants that acetylation at K314 and K315 in addition to acetylation of K122 and K123 negatively regulate p65 functions at inflammatory target genes. Of note, detection of acetylation of p65 requires overexpression of HATs and p65 (Figure 4), suggesting that acetylation is a low abundant and transient event that affects only a fraction of all p65 protein present in the cell.

HDAC3 can be found in the cytosol and in the nucleus (28), but the subcellular compartment for HDAC3-mediated regulation of the p65 acetylation status is presently not known. Our data show that most of the HDAC3 protein in epithelial cells is found in the nucleus (Figure 6B) but does not stably associate with chromatin (Figure 6C). Moreover, a DNA-binding defective p65 point mutant (p65 E39I) is still deacetylated by HDAC3 (Supplementary Figure S8), arguing that deacetylation must not necessarily occur at chromatin-bound p65. Like most classical HDACs, HDAC3 is contained in large high molecular weight co-repressor complexes of up to 1–2 MDa (21,23,25,26). HDAC5 and HDAC8 did not deacetylate p65 in our assay systems, whereas HDAC1 and HDAC2 also deacetylated p65 at lysines K314 or K315 (Supplementary Figure S9). As knockdown of HDAC1 and HDAC2 also impairs IL-1-inducible *Cxcl2*

expression (Supplementary Figure S10), it will be interesting to define the individual roles of other regulators of p65 acetylation for gene expression in future studies. Of note, we also observed HDAC3-regulated genes, which are not p65-dependent (Supplementary Table S1), thus showing that HDAC3 operates also by further p65-independent mechanisms.

During the course of this study, we also noted that IL-1-induced genes were more strongly affected by HDAC3 suppression than TNF-induced genes (Supplementary Figure S11). IL-1 and TNF activate overlapping sets of proinflammatory genes and share many signaling components, but emerging evidence also suggests specific pathways as exemplified by usage of different E2 and E3 ubiquitination enzymes in their NF- κ B activating pathways (58). It will therefore be interesting to clarify a specific role of HDAC3 in cytokine pathways in future studies.

In line with emerging functions of HDAC3 in innate immunity, deletion of the enzyme in macrophages was recently shown to affect histone acetylation leading to the expression of a set of IL-4-regulated genes. These findings demonstrate a specific role of HDAC3 in controlling macrophage polarization involving epigenetic mechanisms (59). Our study now reveals an unexpected role of HDAC3 for the control of IL-1-triggered pro-inflammatory gene expression. Apparently, the IL-1 pathway directs the recruitment of HDAC3 into gene-regulatory complexes distinct from the known co-repressor complexes. At present, the nature of these co-activator complexes is unknown and may not require stable association with chromatin. This non-epigenetic effect is of biomedical relevance, as non-selective HDAC inhibitors are used as anti-cancer drugs and are currently tested in a number of clinical trials for the treatment of further diseases (46,60). As an example, clinical data show anti-inflammatory properties of HDAC inhibitors that can be used for the treatment of graft versus host disease (61). In addition, animal models have revealed strong anti-inflammatory effects by pharmacological modulators of HDAC activity (62). HDAC inhibitors show antiphlogistic efficacy in models of inflammatory bowel disease (63) and of rheumatoid arthritis (64). Chemokines such as IL-8 or CXCL2 mediate leukocyte trafficking, leukocyte infiltration, angiogenesis or metastasis (65–67). Hence, IL-1-driven signaling mechanisms, which control the magnitude and kinetics of expression of these chemokines are important modulators of disease processes. By demonstrating a general role of HDAC3 in positive regulation of IL-1 responses at the cellular level, this study contributes novel insights into the molecular mechanisms underlying anti-inflammatory effects of HDAC inhibition.

SUPPLEMENTARY DATA

Supplementary Data are available at NAR Online: Supplementary Tables 1–3, Supplementary Figures 1–11 and Supplementary Materials & Methods.

FUNDING

Deutsche Forschungsgemeinschaft (DFG) [Kr1143/5-3 and Kr1143/7-1] and [SFB566/Z02 and TRR81/B2]; [SCHM 1417/4-2, SCHM 1417/7-1, SCHM 1417/8-1, GRK 1566/1 to M.L.S.]; Deutscher akademischer Austauschdienst [A/08/98404 to M.L.S.]; Work from both laboratories is further supported by the Excellence Cluster Cardio-Pulmonary System (ECCPS), the LOEWE/UGMLC program and [SFB/TRR81] NIH [R01 DK073639 to E.B.]; CCFA [SRA 2737]. Funding for open access charge: DFG.

Conflict of interest statement. None declared.

REFERENCES

- Gaestel, M., Kotlyarov, A. and Kracht, M. (2009) Targeting innate immunity protein kinase signalling in inflammation. *Nat. Rev. Drug Discov.*, **8**, 480–499.
- Smale, S.T. (2011) Hierarchies of NF-kappaB target-gene regulation. *Nat. Immunol.*, **12**, 689–694.
- Hayden, M.S. and Ghosh, S. (2008) Shared principles in NF-kappaB signaling. *Cell*, **132**, 344–362.
- Perkins, N.D. (2012) The diverse and complex roles of NF-kappaB subunits in cancer. *Nat. Rev. Cancer*, **12**, 121–132.
- Schmitz, M.L., Mattioli, I., Buss, H. and Kracht, M. (2004) NF-kappaB: a multifaceted transcription factor regulated at several levels. *ChemBiochem.*, **5**, 1348–1358.
- O'Shea, J.M. and Perkins, N.D. (2008) Regulation of the RelA (p65) transactivation domain. *Biochem. Soc. Trans.*, **36**, 603–608.
- Wietek, C. and O'Neill, L.A. (2007) Diversity and regulation in the NF-kappaB system. *Trends Biochem. Sci.*, **32**, 311–319.
- Calao, M., Burny, A., Quivy, V., Dekoninck, A. and van Lint, C. (2008) A pervasive role of histone acetyltransferases and deacetylases in an NF-kappaB-signaling code. *Trends Biochem. Sci.*, **33**, 339–349.
- Kiernan, R., Bres, V., Ng, R.W., Coudart, M.P., El Messaoudi, S., Sardet, C., Jin, D.Y., Emiliani, S. and Benkirane, M. (2003) Post-activation turn-off of NF-kappa B-dependent transcription is regulated by acetylation of p65. *J. Biol. Chem.*, **278**, 2758–2766.
- Chen, L.F., Williams, S.A., Mu, Y., Nakano, H., Duerr, J.M., Buckbinder, L. and Greene, W.C. (2005) NF-kappaB RelA phosphorylation regulates RelA acetylation. *Mol. Cell. Biol.*, **25**, 7966–7975.
- Chen, L.F. and Greene, W.C. (2003) Regulation of distinct biological activities of the NF-kappaB transcription factor complex by acetylation. *J. Mol. Med.*, **81**, 549–557.
- Buerki, C., Rothgiesser, K.M., Valovka, T., Owen, H.R., Rehrauer, H., Fey, M., Lane, W.S. and Hottiger, M.O. (2008) Functional relevance of novel p300-mediated lysine 314 and 315 acetylation of RelA/p65. *Nucleic Acids Res.*, **36**, 1665–1680.
- Rothgiesser, K.M., Erener, S., Waibel, S., Luscher, B. and Hottiger, M.O. (2010) SIRT2 regulates NF-kappaB dependent gene expression through deacetylation of p65 Lys310. *J. Cell. Sci.*, **123**, 4251–4258.
- Rothgiesser, K.M., Fey, M. and Hottiger, M.O. (2010) Acetylation of p65 at lysine 314 is important for late NF-kappaB-dependent gene expression. *BMC Genomics*, **11**, 22.
- Li, H., Wittwer, T., Weber, A., Schneider, H., Moreno, R., Maine, G.N., Kracht, M., Schmitz, M.L. and Burstein, E. (2012) Regulation of NF-kappaB activity by competition between RelA acetylation and ubiquitination. *Oncogene*, **31**, 611–623.
- Chen, L., Fischle, W., Verdin, E. and Greene, W.C. (2001) Duration of nuclear NF-kappaB action regulated by reversible acetylation. *Science*, **293**, 1653–1657.
- Furia, B., Deng, L., Wu, K., Baylor, S., Kehn, K., Li, H., Donnelly, R., Coleman, T. and Kashanchi, F. (2002) Enhancement of nuclear factor-kappa B acetylation by coactivator p300 and HIV-1 Tat proteins. *J. Biol. Chem.*, **277**, 4973–4980.
- Zhong, H., May, M.J., Jimi, E. and Ghosh, S. (2002) The phosphorylation status of nuclear NF-kappa B determines its association with CBP/p300 or HDAC-1. *Mol. Cell.*, **9**, 625–636.
- Ashburner, B.P., Westerheide, S.D. and Baldwin, A.S. Jr (2001) The p65 (RelA) subunit of NF-kappaB interacts with the histone deacetylase (HDAC) corepressors HDAC1 and HDAC2 to negatively regulate gene expression. *Mol. Cell. Biol.*, **21**, 7065–7077.
- Chen, Y., Wang, H., Yoon, S.O., Xu, X., Hottiger, M.O., Svaren, J., Nave, K.A., Kim, H.A., Olson, E.N. and Lu, Q.R. (2011) HDAC-mediated deacetylation of NF-kappaB is critical for Schwann cell myelination. *Nat. Neurosci.*, **14**, 437–441.
- Yang, X.J. and Seto, E. (2008) The Rpd3/Hda1 family of lysine deacetylases: from bacteria and yeast to mice and men. *Nat. Rev. Mol. Cell. Biol.*, **9**, 206–218.
- Yeung, F., Hoberg, J.E., Ramsey, C.S., Keller, M.D., Jones, D.R., Frye, R.A. and Mayo, M.W. (2004) Modulation of NF-kappaB-dependent transcription and cell survival by the SIRT1 deacetylase. *EMBO J.*, **23**, 2369–2380.
- Wen, Y.D., Perissi, V., Staszewski, L.M., Yang, W.M., Krones, A., Glass, C.K., Rosenfeld, M.G. and Seto, E. (2000) The histone deacetylase-3 complex contains nuclear receptor corepressors. *Proc. Natl Acad. Sci. USA*, **97**, 7202–7207.
- Emiliani, S., Fischle, W., van Lint, C., Al Abed, Y. and Verdin, E. (1998) Characterization of a human RPD3 ortholog, HDAC3. *Proc. Natl Acad. Sci. USA*, **95**, 2795–2800.
- Li, J., Wang, J., Wang, J., Nawaz, Z., Liu, J.M., Qin, J. and Wong, J. (2000) Both corepressor proteins SMRT and N-CoR exist in large protein complexes containing HDAC3. *EMBO J.*, **19**, 4342–4350.
- Guenther, M.G., Lane, W.S., Fischle, W., Verdin, E., Lazar, M.A. and Shiekhattar, R. (2000) A core SMRT corepressor complex containing HDAC3 and TBL1, a WD40-repeat protein linked to deafness. *Genes Dev.*, **14**, 1048–1057.
- Karagianni, P. and Wong, J. (2007) HDAC3: taking the SMRT-N-CoR road to repression. *Oncogene*, **26**, 5439–5449.
- Yang, W.M., Tsai, S.C., Wen, Y.D., Fejer, G. and Seto, E. (2002) Functional domains of histone deacetylase-3. *J. Biol. Chem.*, **277**, 9447–9454.
- Bhaskara, S. and Hiebert, S.W. (2011) Role for histone deacetylase 3 in maintenance of genome stability. *Cell Cycle*, **10**, 727–728.
- Bhaskara, S., Knutson, S.K., Jiang, G., Chandrasekharan, M.B., Wilson, A.J., Zheng, S., Yenamandra, A., Locke, K., Yuan, J.L., Bonine-Summers, A.R. et al. (2010) Hdac3 is essential for the maintenance of chromatin structure and genome stability. *Cancer Cell*, **18**, 436–447.
- Montgomery, R.L., Potthoff, M.J., Haberland, M., Qi, X., Matsuzaki, S., Humphries, K.M., Richardson, J.A., Bassel-Duby, R. and Olson, E.N. (2008) Maintenance of cardiac energy metabolism by histone deacetylase 3 in mice. *J. Clin. Invest.*, **118**, 3588–3597.
- Knutson, S.K., Chyla, B.J., Amann, J.M., Bhaskara, S., Huppert, S.S. and Hiebert, S.W. (2008) Liver-specific deletion of histone deacetylase 3 disrupts metabolic transcriptional networks. *EMBO J.*, **27**, 1017–1028.
- Bhaskara, S., Chyla, B.J., Amann, J.M., Knutson, S.K., Cortez, D., Sun, Z.W. and Hiebert, S.W. (2008) Deletion of histone deacetylase 3 reveals critical roles in S phase progression and DNA damage control. *Mol. Cell.*, **30**, 61–72.
- Dinarello, C.A., Fossati, G. and Maccagnani, P. (2011) Histone deacetylase inhibitors for treating a spectrum of diseases not related to cancer. *Mol. Med.*, **17**, 333–352.
- Thiefes, A., Wolf, A., Doerrie, A., Grassl, G.A., Matsumoto, K., Autenrieth, I., Bohn, E., Sakurai, H., Niedenthal, R., Resch, K. et al. (2006) The *Yersinia enterocolitica* effector YopP inhibits host cell signalling by inactivating the protein kinase TAK1 in the IL-1 signalling pathway. *EMBO Rep.*, **7**, 838–844.
- Hoffmann, E., Thiefes, A., Buhrow, D., Dittrich-Breiholz, O., Schneider, H., Resch, K. and Kracht, M. (2005) MEK1-dependent delayed expression of Fos-related antigen-1 counteracts c-Fos and p65 NF-kappaB-mediated interleukin-8 transcription in response to cytokines or growth factors. *J. Biol. Chem.*, **280**, 9706–9718.
- Shi, Y., Kotlyarov, A., Laabeta, K., Gruber, A.D., Butt, E., Marcus, K., Meyer, H.E., Friedrich, A., Volk, H.D. and Gaestel, M. (2003) Elimination of protein kinase MK5/PRAK activity by

- targeted homologous recombination. *Mol. Cell. Biol.*, **23**, 7732–7741.
38. Alenghat, T., Meyers, K., Mullican, S.E., Leitner, K., Adeniji-Adele, A., Avila, J., Bucan, M., Ahima, R.S., Kaestner, K.H. and Lazar, M.A. (2008) Nuclear receptor corepressor and histone deacetylase 3 govern circadian metabolic physiology. *Nature*, **456**, 997–1000.
 39. Holtmann, H., Enninga, J., Kalble, S., Thiefes, A., Dorrie, A., Broemer, M., Winzen, R., Wilhelm, A., Ninomiya-Tsuji, J., Matsumoto, K. *et al.* (2001) The MAPK kinase kinase TAK1 plays a central role in coupling the interleukin-1 receptor to both transcriptional and RNA-targeted mechanisms of gene regulation. *J. Biol. Chem.*, **276**, 3508–3516.
 40. Rzczkowski, K., Beuerlein, K., Muller, H., Dittrich-Breiholz, O., Schneider, H., Kettner-Buhrow, D., Holtmann, H. and Kracht, M. (2011) c-Jun N-terminal kinase phosphorylates DCP1a to control formation of P bodies. *J. Cell. Biol.*, **194**, 581–596.
 41. de la Vega, L., Grishina, I., Moreno, R., Kruger, M., Braun, T. and Schmitz, M.L. (2012) A redox-regulated SUMO/acylation switch of HIPK2 controls the survival threshold to oxidative stress. *Mol. Cell.*, **46**, 472–483.
 42. Hu, E., Chen, Z., Fredrickson, T., Zhu, Y., Kirkpatrick, R., Zhang, G.F., Johanson, K., Sung, C.M., Liu, R. and Winkler, J. (2000) Cloning and characterization of a novel human class I histone deacetylase that functions as a transcription repressor. *J. Biol. Chem.*, **275**, 15254–15264.
 43. Tanaka, T., Grusby, M.J. and Kaisho, T. (2007) PDLIM2-mediated termination of transcription factor NF-kappaB activation by intranuclear sequestration and degradation of the p65 subunit. *Nat. Immunol.*, **8**, 584–591.
 44. Saeed, A.I., Sharov, V., White, J., Li, J., Liang, W., Bhagabati, N., Braisted, J., Klapa, M., Currier, T., Thiagarajan, M. *et al.* (2003) TM4: a free, open-source system for microarray data management and analysis. *Biotechniques*, **34**, 374–378.
 45. Wolter, S., Doerrie, A., Weber, A., Schneider, H., Hoffmann, E., von der, O.J., Bakiri, L., Wagner, E.F., Resch, K. and Kracht, M. (2008) c-Jun controls histone modifications, NF-kappaB recruitment, and RNA polymerase II function to activate the ccl2 gene. *Mol. Cell. Biol.*, **28**, 4407–4423.
 46. Bolden, J.E., Peart, M.J. and Johnstone, R.W. (2006) Anticancer activities of histone deacetylase inhibitors. *Nat. Rev. Drug Discov.*, **5**, 769–784.
 47. Yoshida, M., Kijima, M., Akita, M. and Beppu, T. (1990) Potent and specific inhibition of mammalian histone deacetylase both in vivo and in vitro by trichostatin A. *J. Biol. Chem.*, **265**, 17174–17179.
 48. de Ruijter, A.J., van Gennip, A.H., Caron, H.N., Kemp, S. and van Kuilenburg, A.B. (2003) Histone deacetylases (HDACs): characterization of the classical HDAC family. *Biochem. J.*, **370**, 737–749.
 49. Gupta, P., Ho, P.C., Ha, S.G., Lin, Y.W. and Wei, L.N. (2009) HDAC3 as a molecular chaperone for shuttling phosphorylated TR2 to PML: a novel deacetylase activity-independent function of HDAC3. *PLoS One*, **4**, e4363.
 50. Wang, J., Mahmud, S.A., Bitterman, P.B., Huo, Y. and Slungaard, A. (2007) Histone deacetylase inhibitors suppress TF-kappaB-dependent agonist-driven tissue factor expression in endothelial cells and monocytes. *J. Biol. Chem.*, **282**, 28408–28418.
 51. Khan, N., Jeffers, M., Kumar, S., Hackett, C., Boldog, F., Khramtsov, N., Qian, X., Mills, E., Berghs, S.C., Carey, N. *et al.* (2008) Determination of the class and isoform selectivity of small-molecule histone deacetylase inhibitors. *Biochem. J.*, **409**, 581–589.
 52. Wang, Z., Zang, C., Cui, K., Schones, D.E., Barski, A., Peng, W. and Zhao, K. (2009) Genome-wide mapping of HATs and HDACs reveals distinct functions in active and inactive genes. *Cell.*, **138**, 1019–1031.
 53. Hoffmann, A., Leung, T.H. and Baltimore, D. (2003) Genetic analysis of NF-kappaB/Rel transcription factors defines functional specificities. *EMBO J.*, **22**, 5530–5539.
 54. Moreno, R., Sobotzik, J.M., Schultz, C. and Schmitz, M.L. (2010) Specification of the NF-kappaB transcriptional response by p65 phosphorylation and TNF-induced nuclear translocation of IKK epsilon. *Nucleic Acids Res.*, **38**, 6029–6044.
 55. Geng, H., Wittwer, T., Dittrich-Breiholz, O., Kracht, M. and Schmitz, M.L. (2009) Phosphorylation of NF-kappaB p65 at Ser468 controls its COMMD1-dependent ubiquitination and target gene-specific proteasomal elimination. *EMBO Rep.*, **10**, 381–386.
 56. Huang, B., Yang, X.D., Zhou, M.M., Ozato, K. and Chen, L.F. (2009) Brd4 coactivates transcriptional activation of NF-kappaB via specific binding to acetylated RelA. *Mol. Cell. Biol.*, **29**, 1375–1387.
 57. Hoberg, J.E., Yeung, F. and Mayo, M.W. (2004) SMRT derepression by the IkappaB kinase alpha: a prerequisite to NF-kappaB transcription and survival. *Mol. Cell.*, **16**, 245–255.
 58. Liu, S. and Chen, Z.J. (2011) Expanding role of ubiquitination in NF-kappaB signaling. *Cell. Res.*, **21**, 6–21.
 59. Mullican, S.E., Gaddis, C.A., Alenghat, T., Nair, M.G., Giacomini, P.R., Everett, L.J., Feng, D., Steger, D.J., Schug, J., Artis, D. *et al.* (2011) Histone deacetylase 3 is an epigenomic brake in macrophage alternative activation. *Genes Dev.*, **25**, 2480–2488.
 60. Shakespear, M.R., Halili, M.A., Irvine, K.M., Fairlie, D.P. and Sweet, M.J. (2011) Histone deacetylases as regulators of inflammation and immunity. *Trends Immunol.*, **32**, 335–343.
 61. Choi, S. and Reddy, P. (2011) HDAC inhibition and graft versus host disease. *Mol. Med.*, **17**, 404–416.
 62. Grabiec, A.M., Tak, P.P. and Reedquist, K.A. (2011) Function of histone deacetylase inhibitors in inflammation. *Crit. Rev. Immunol.*, **31**, 233–263.
 63. Edwards, A.J. and Pender, S.L. (2011) Histone deacetylase inhibitors and their potential role in inflammatory bowel diseases. *Biochem. Soc. Trans.*, **39**, 1092–1095.
 64. Grabiec, A.M., Korchynski, O., Tak, P.P. and Reedquist, K.A. (2012) Histone deacetylase inhibitors suppress rheumatoid arthritis fibroblast-like synoviocyte and macrophage IL-6 production by accelerating mRNA decay. *Ann. Rheum. Dis.*, **71**, 424–431.
 65. Raman, D., Sobolik-Delmaire, T. and Richmond, A. (2011) Chemokines in health and disease. *Exp. Cell. Res.*, **317**, 575–589.
 66. Zlotnik, A., Burkhardt, A.M. and Homey, B. (2011) Homeostatic chemokine receptors and organ-specific metastasis. *Nat. Rev. Immunol.*, **11**, 597–606.
 67. Day, R.B. and Link, D.C. (2012) Regulation of neutrophil trafficking from the bone marrow. *Cell. Mol. Life Sci.*, **69**, 1415–1423.